Supporting information

Proton-induced fluorescence in modified quino[7,8-*h*]quinolines: dual sensing for protons and π-donors

Alexander F. Pozharskii,[a] Valery A. Ozeryanskii,*[a] Vladimir Y. Mikshiev,[a§]
Anatoly V. Chernyshev,[b] Anatoly V. Metelitsa,[b] and Alexander S. Antonov [a§]

[a] *Department of Organic Chemistry, Southern Federal University, Zorge str. 7, 344090 Rostov-on-Don, Russian Federation. E-mail: vv_ozer2@sfedu.ru*
[b] *Institute of Physical and Organic Chemistry, Southern Federal University, Stachki Ave. 194/2, 344090 Rostov-on-Don, Russian Federation*
[§] *Current address: Institute of Chemistry, St. Petersburg State University, Universitetskii pr. 26, 198504 St. Petersburg, Russian Federation*

Table of contents

¹H and ¹³C NMR spectra of new compounds

Figure S1. ¹H NMR spectrum of **5** (CDCl$_3$, 250 MHz).
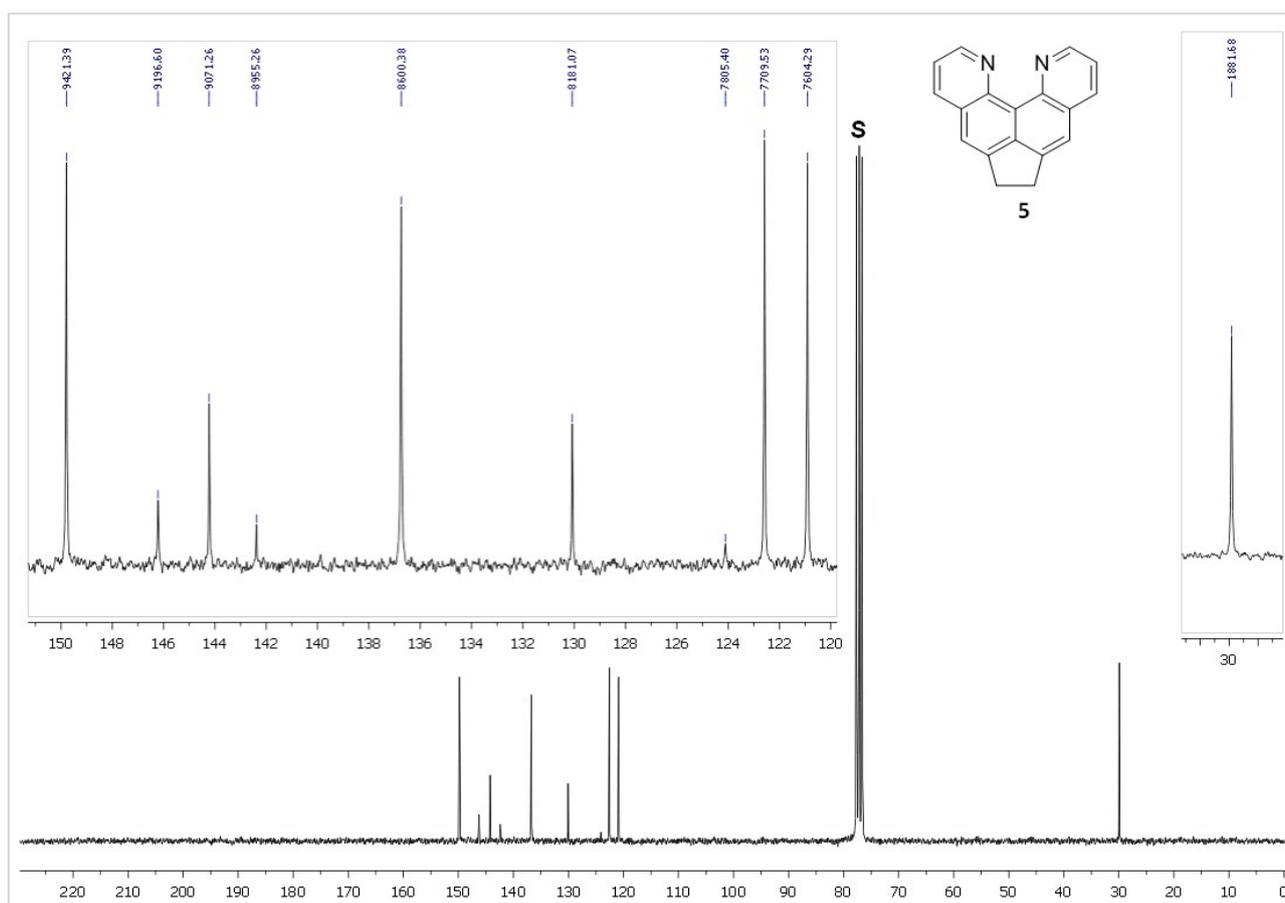
Figure S2. ¹³C NMR spectrum of **5** (CDCl$_3$, 63 MHz).
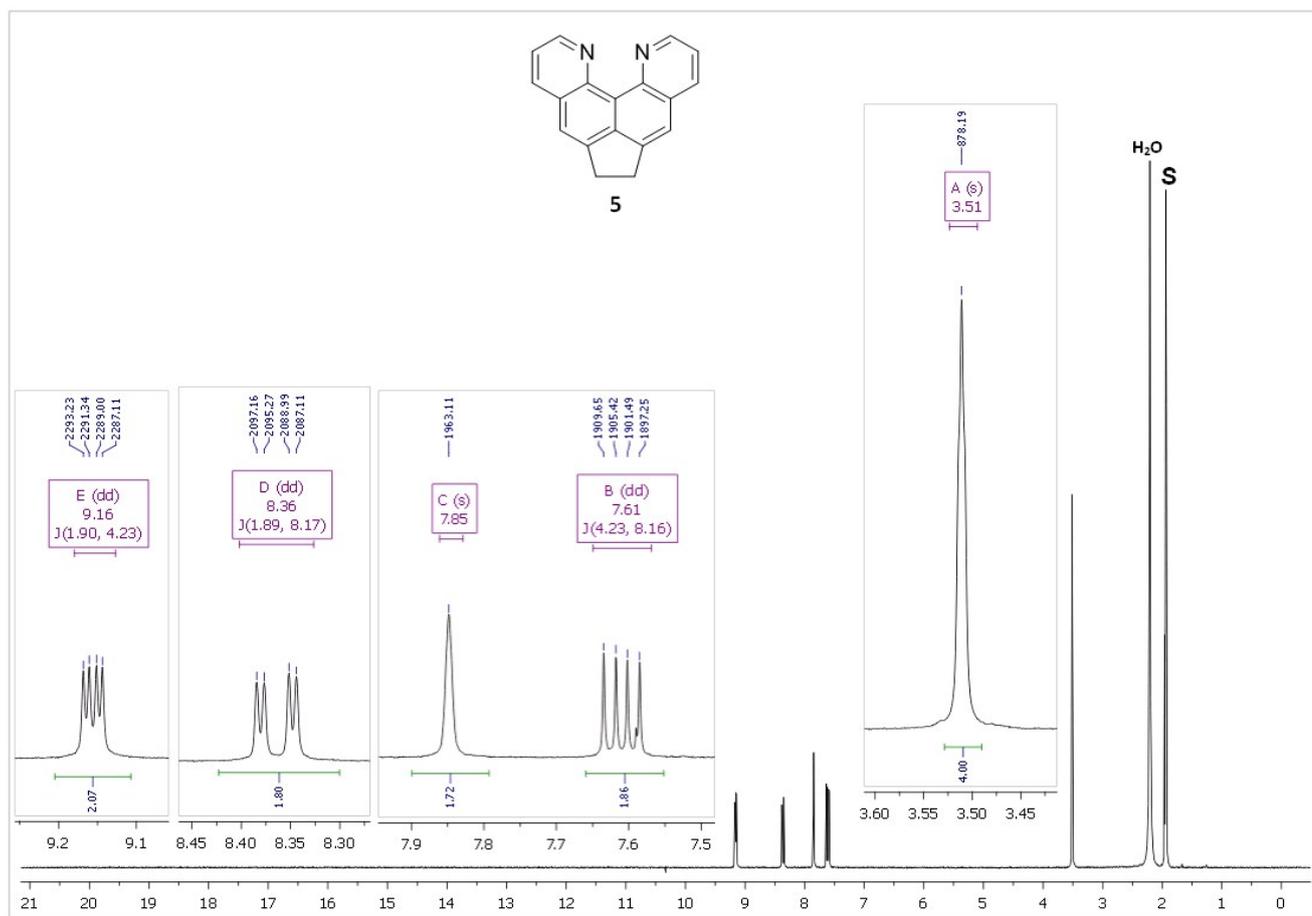
Figure S3. ¹H NMR spectrum of **5** (CD$_3$CN, 250 MHz).
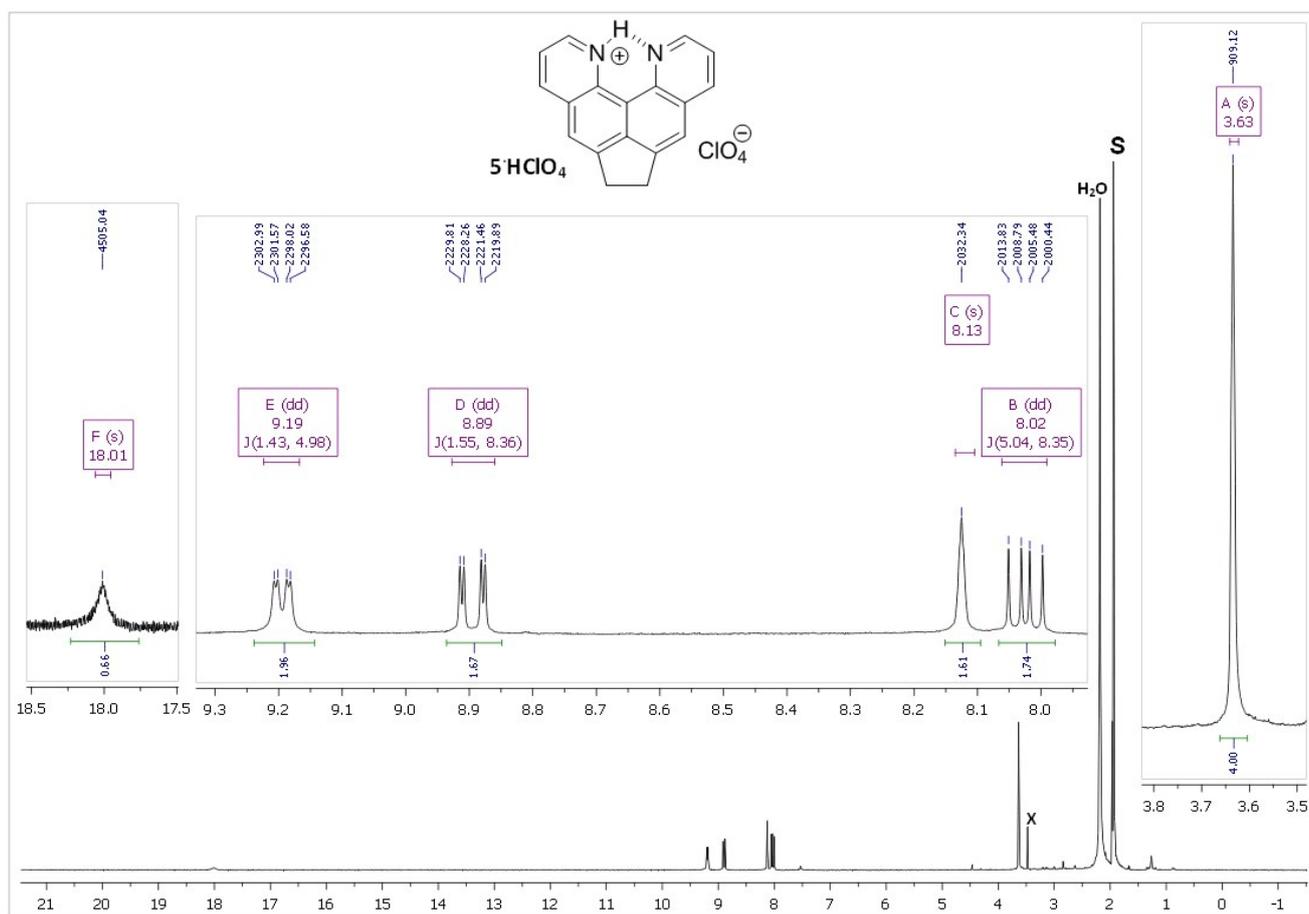

Figure S4. ¹H NMR spectrum of **5·HClO$_4$** (CD$_3$CN, 250 MHz).
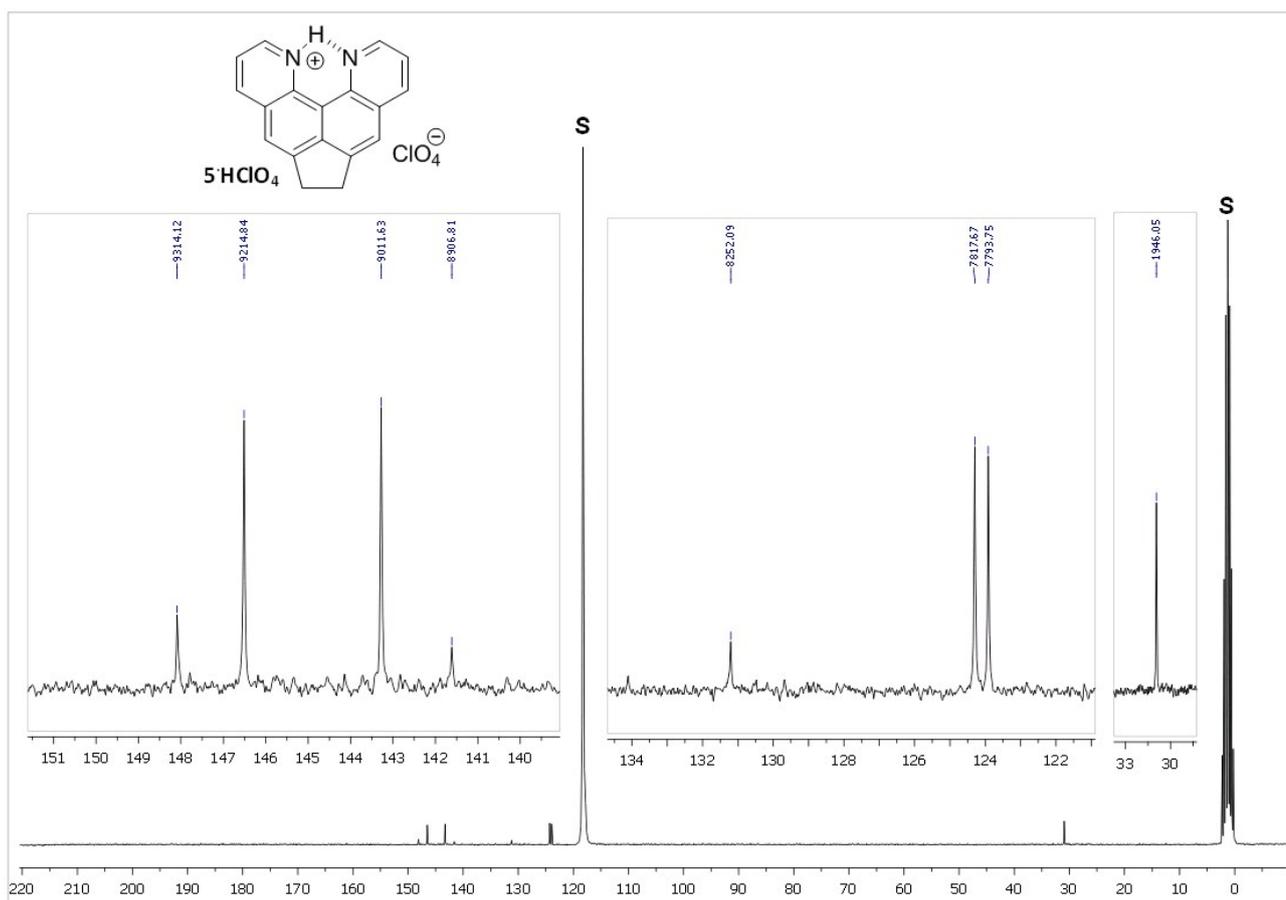
Figure S5. ^{13}C NMR spectrum of **5·HClO$_4$** (CD$_3$CN, 63 MHz).
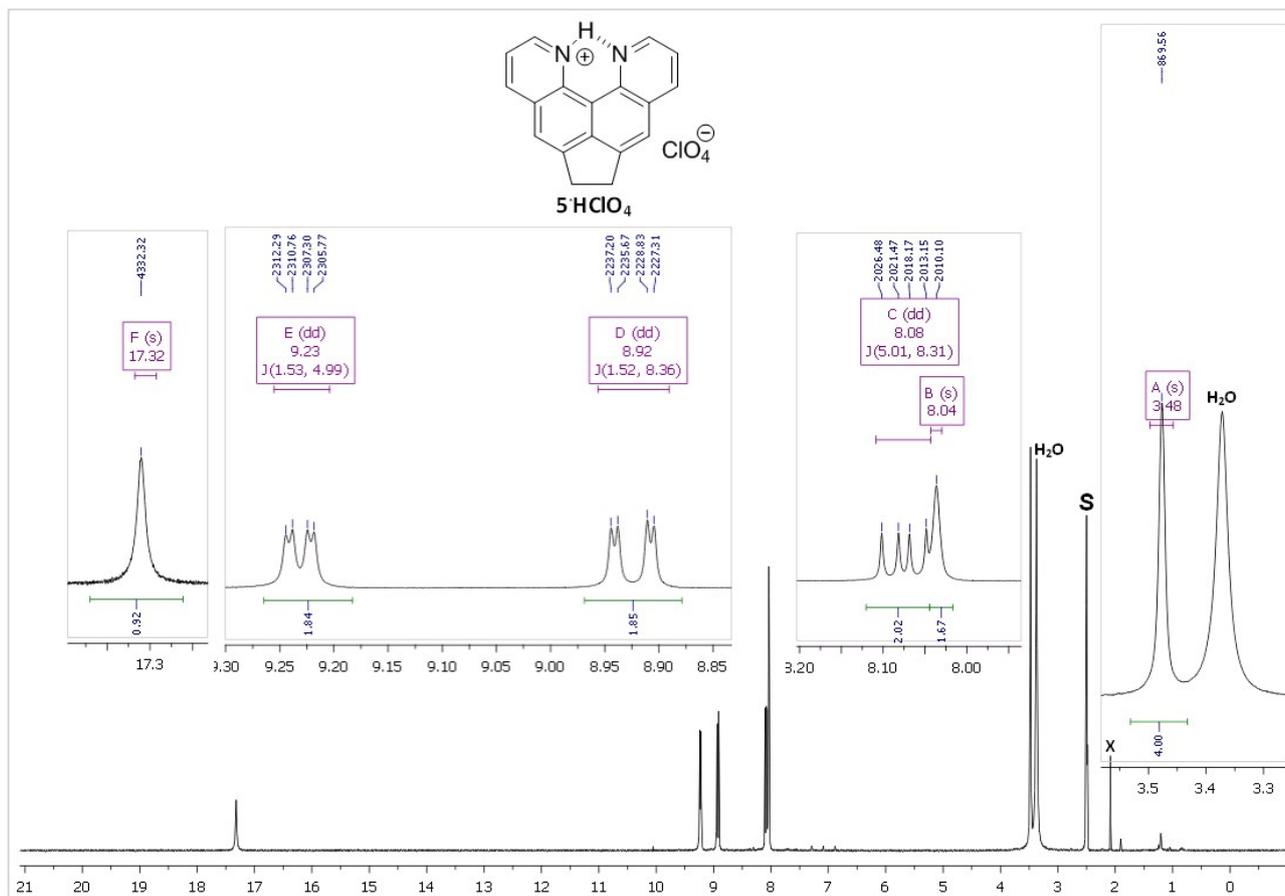
Figure S6. ^1H NMR spectrum of **5·HClO$_4$** (DMSO-d$_6$, 250 MHz).
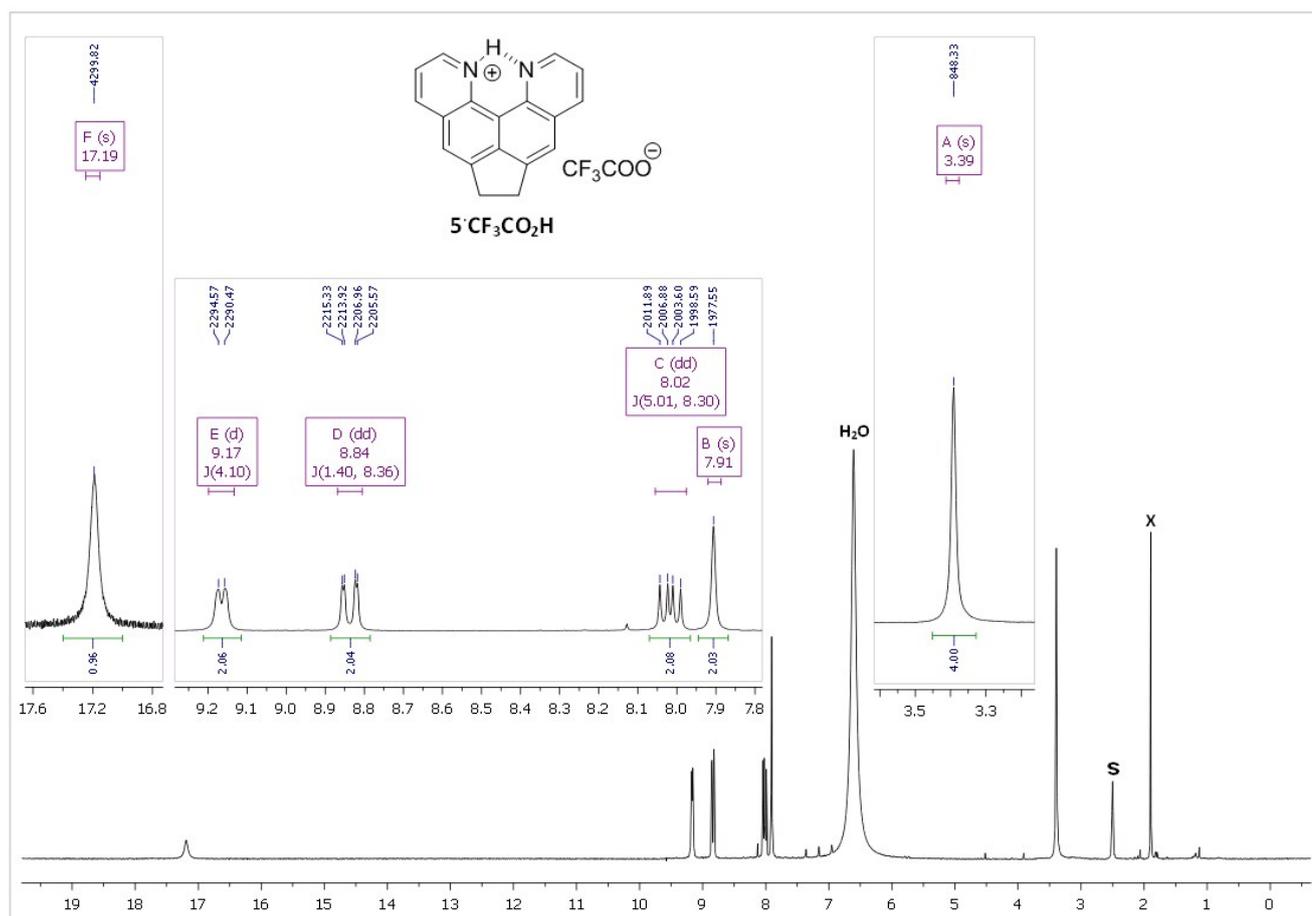
Figure S7. ^{1}H NMR spectrum of **5·CF$_3$CO$_2$H** (DMSO-d$_6$, 250 MHz).
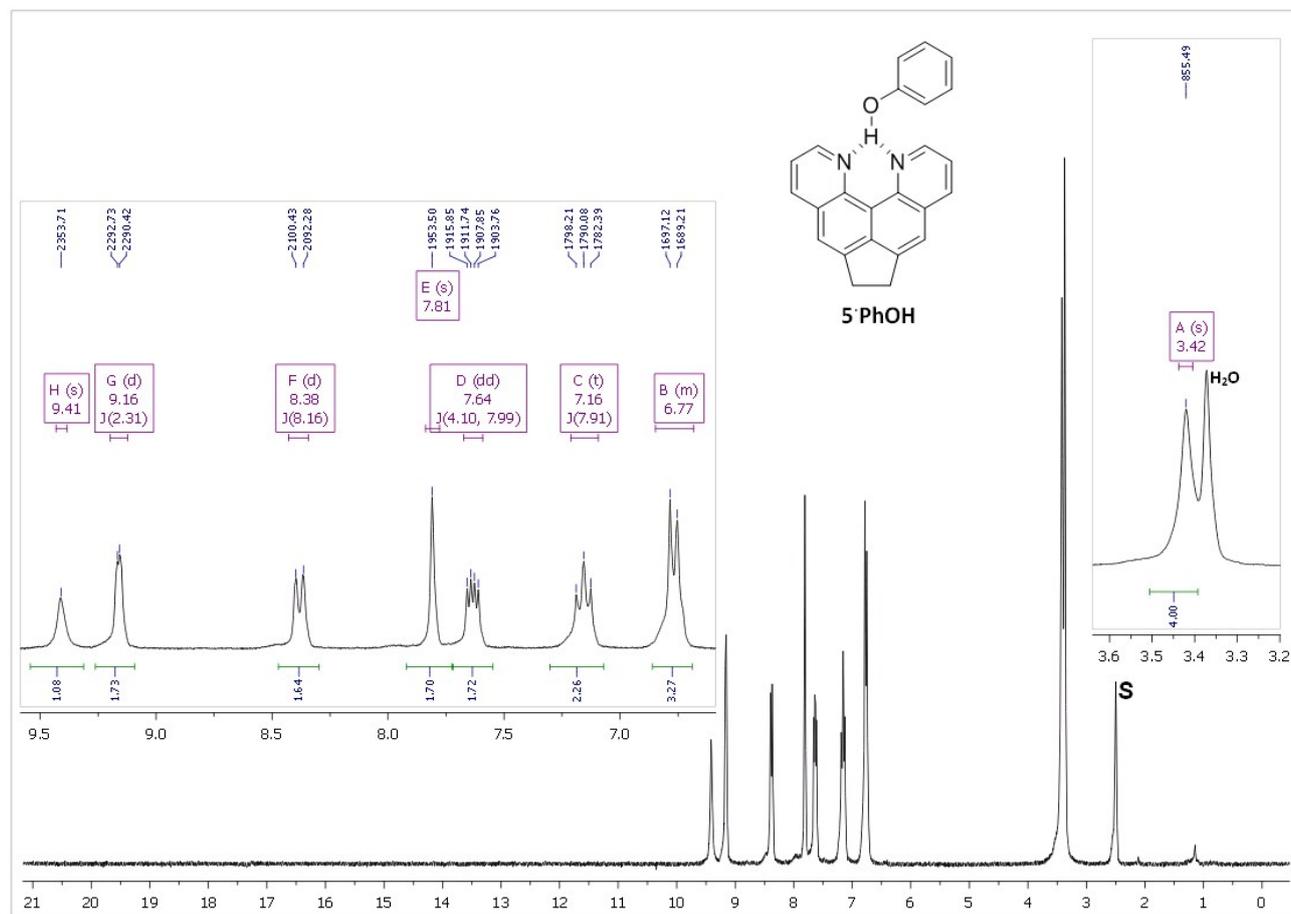
Figure S8. ^{1}H NMR spectrum of **5·PhOH** (DMSO-d$_6$, 250 MHz).
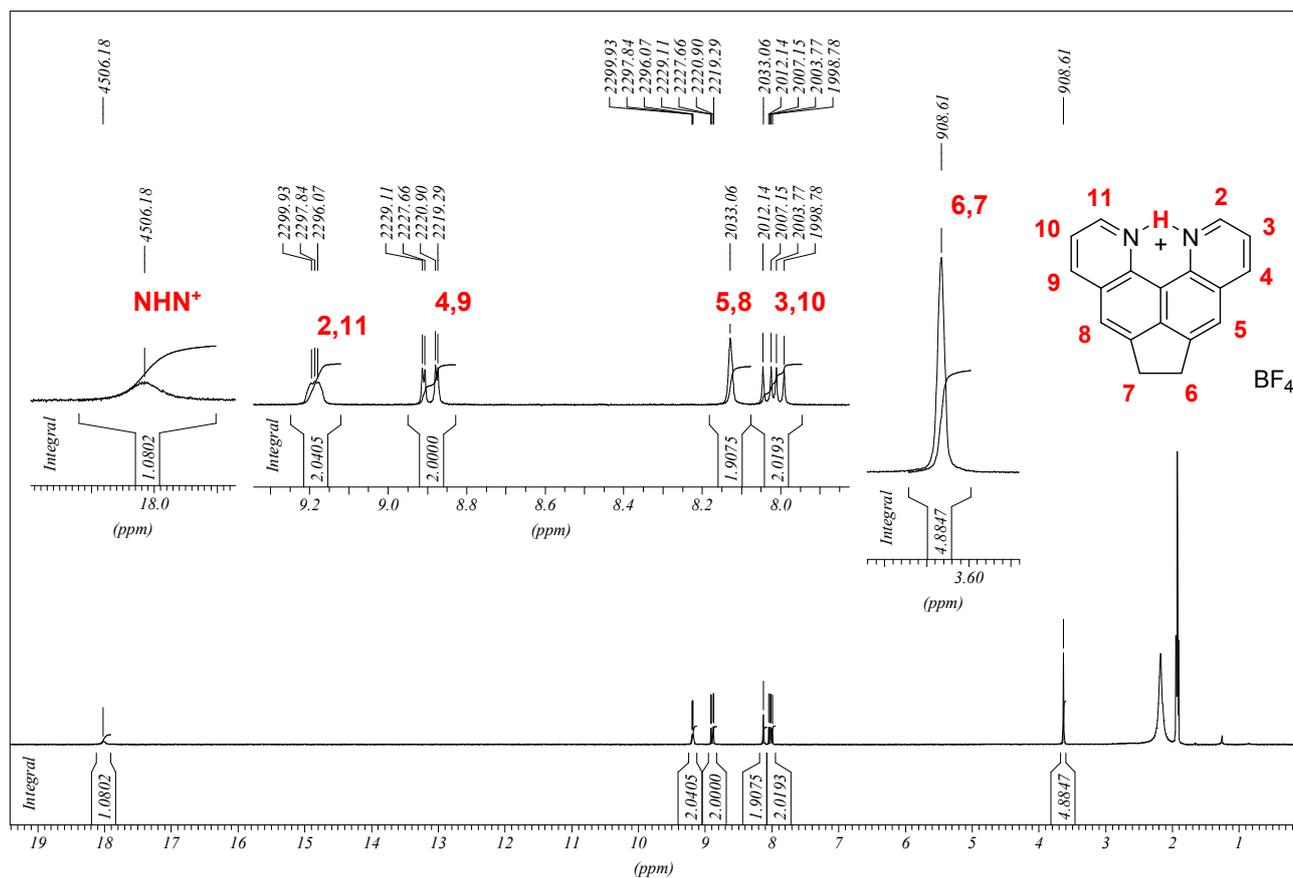
Figure S9. ^{1}H NMR spectrum of salt **5H$^+$BF4$^-$** (CD$_3$CN, 250 MHz).
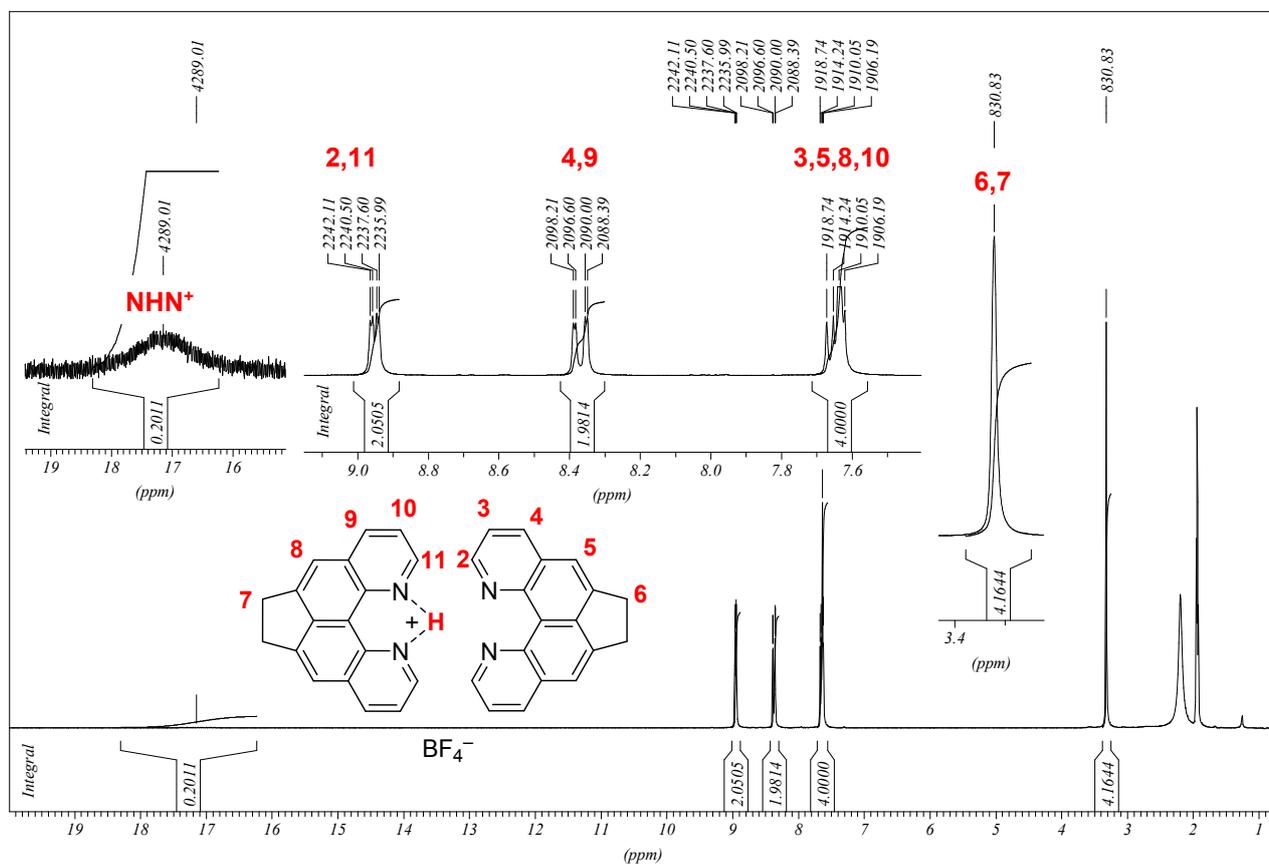
**Figure S10.** ^{1}H NMR spectrum of equimolar mixture of base **5** and its tetrafuoroborate **5H$^+$BF4$^-$** (CD$_3$CN, 250 MHz).

Figure S11. ^{1}H NMR spectrum of equimolar mixture of tetrafuoroborate **5H$^+$BF$_4^-$** and proton sponge **1** with indication of key components (DMSO-d$_6$, 250 MHz).

Figure S12. ^{1}H NMR spectrum of **6a·HBF$_4$** (CD$_3$CN, 250 MHz).
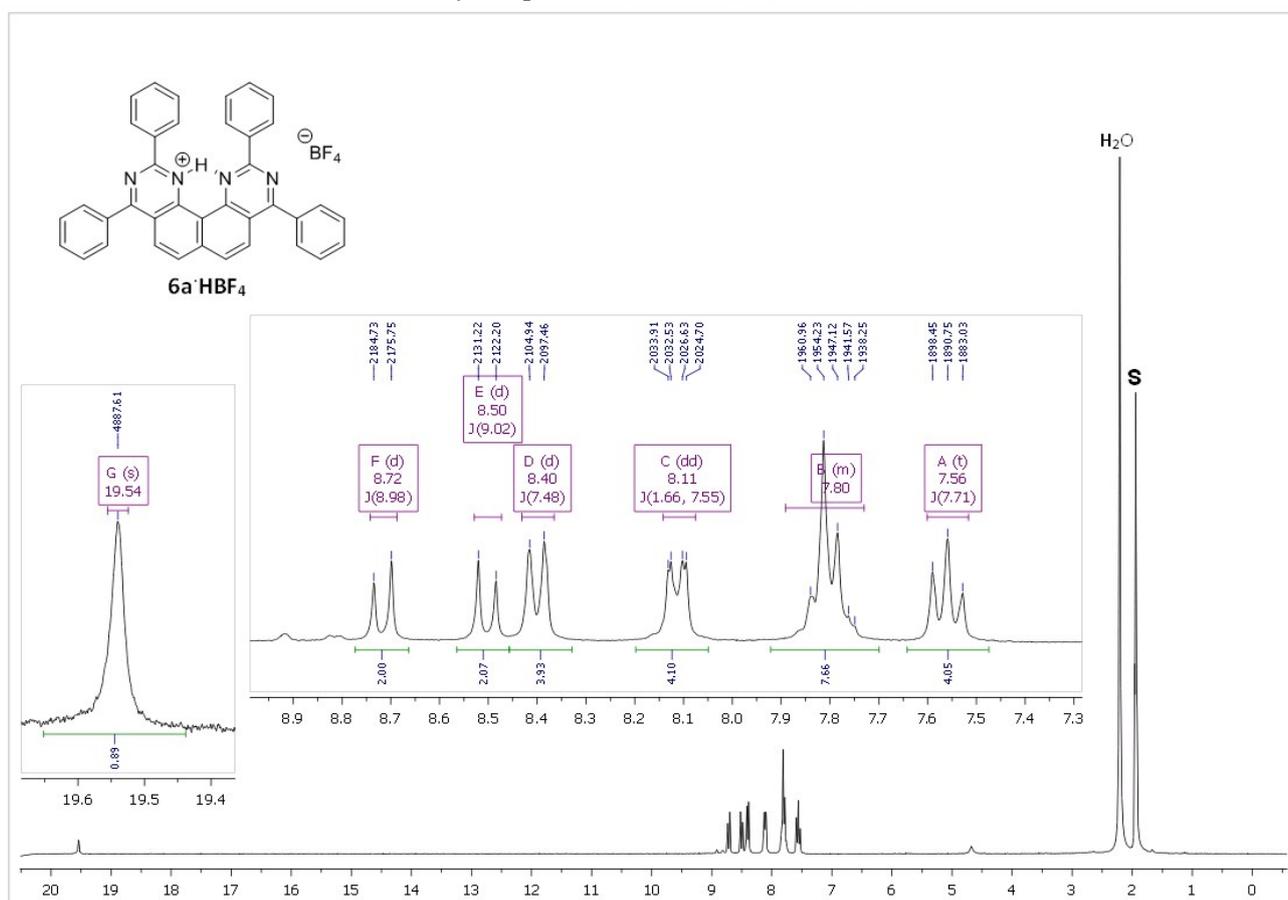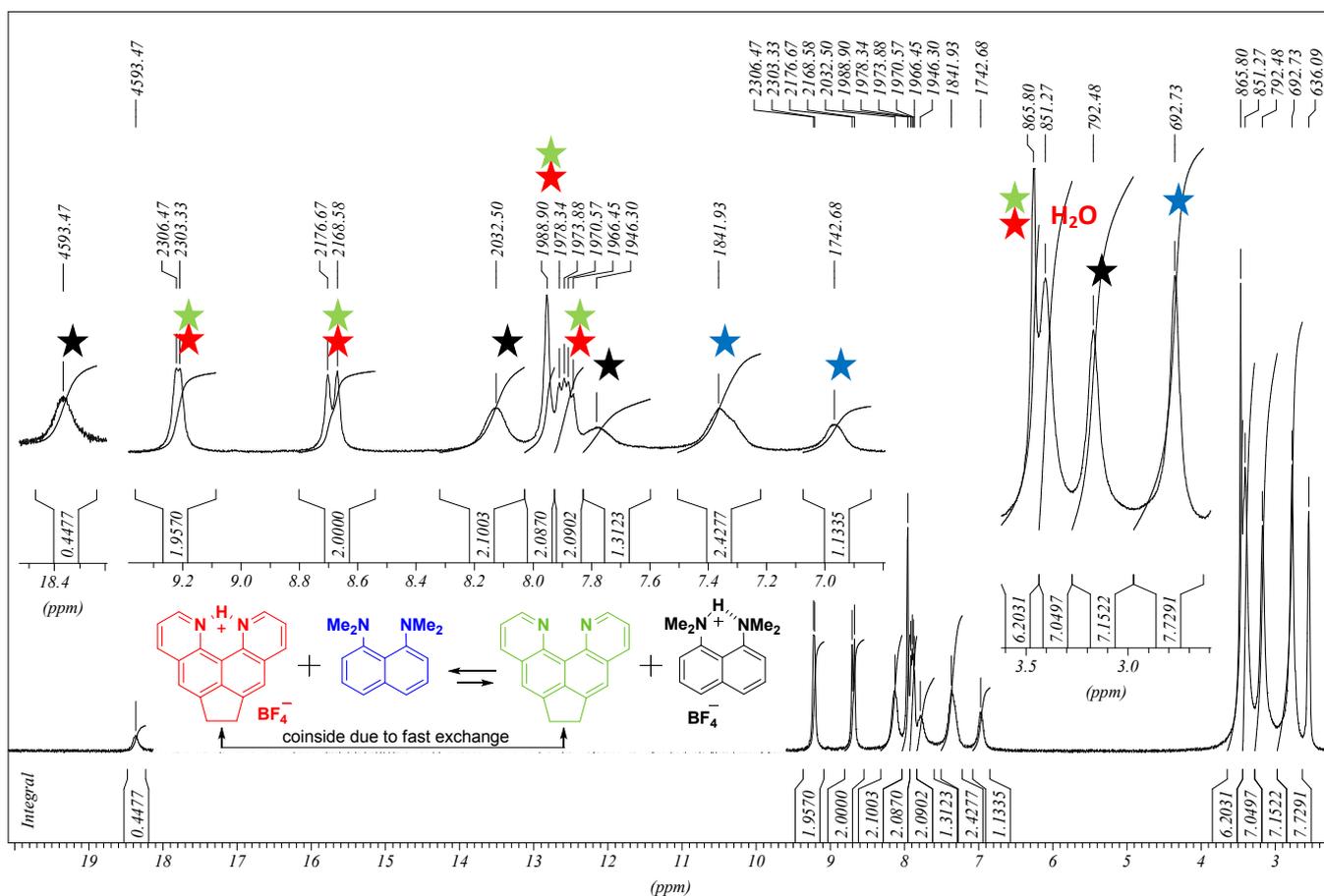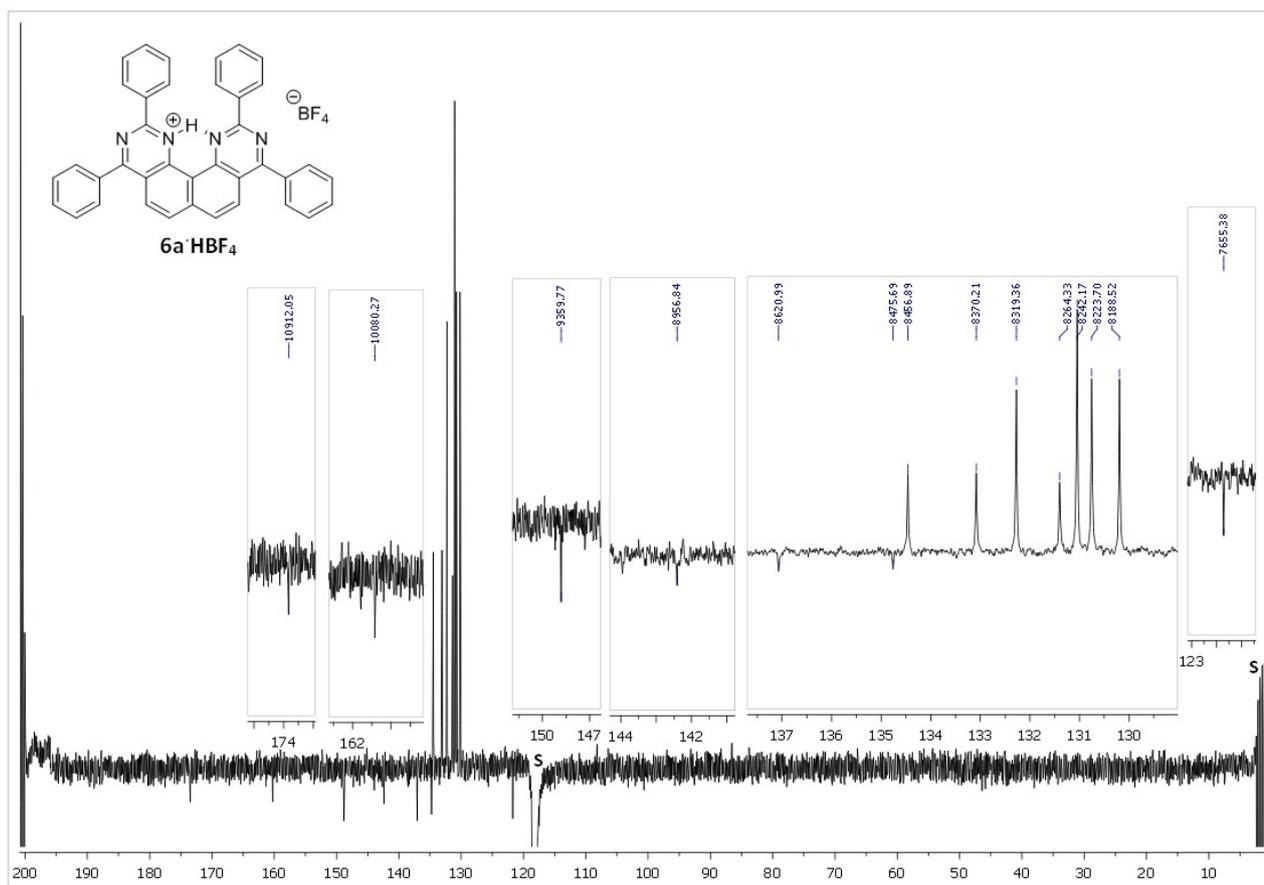
Figure S13. ^{13}C NMR spectrum of **6a·HBF$_4$** (CD$_3$CN, 63 MHz).
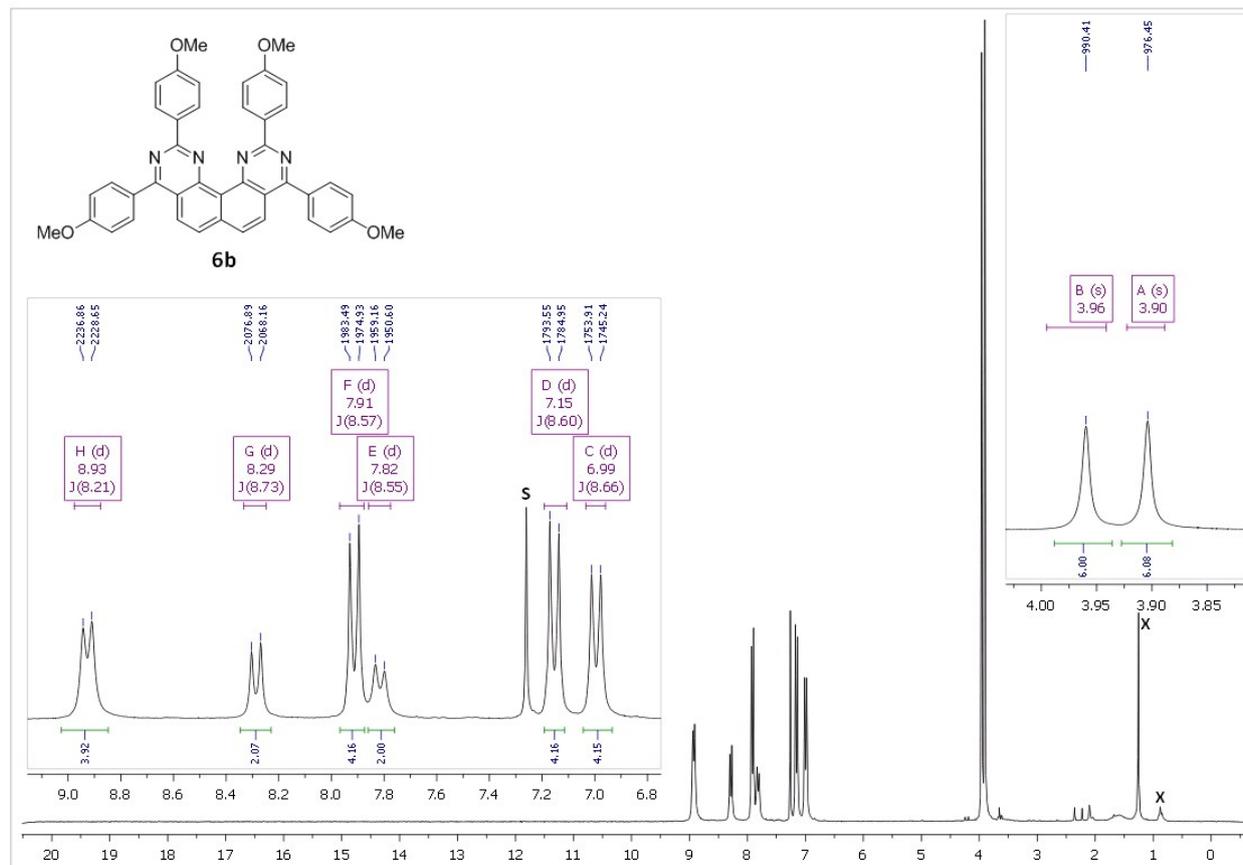
Figure S14. ^{1}H NMR spectrum of **6b** (CDCl$_3$, 250 MHz).
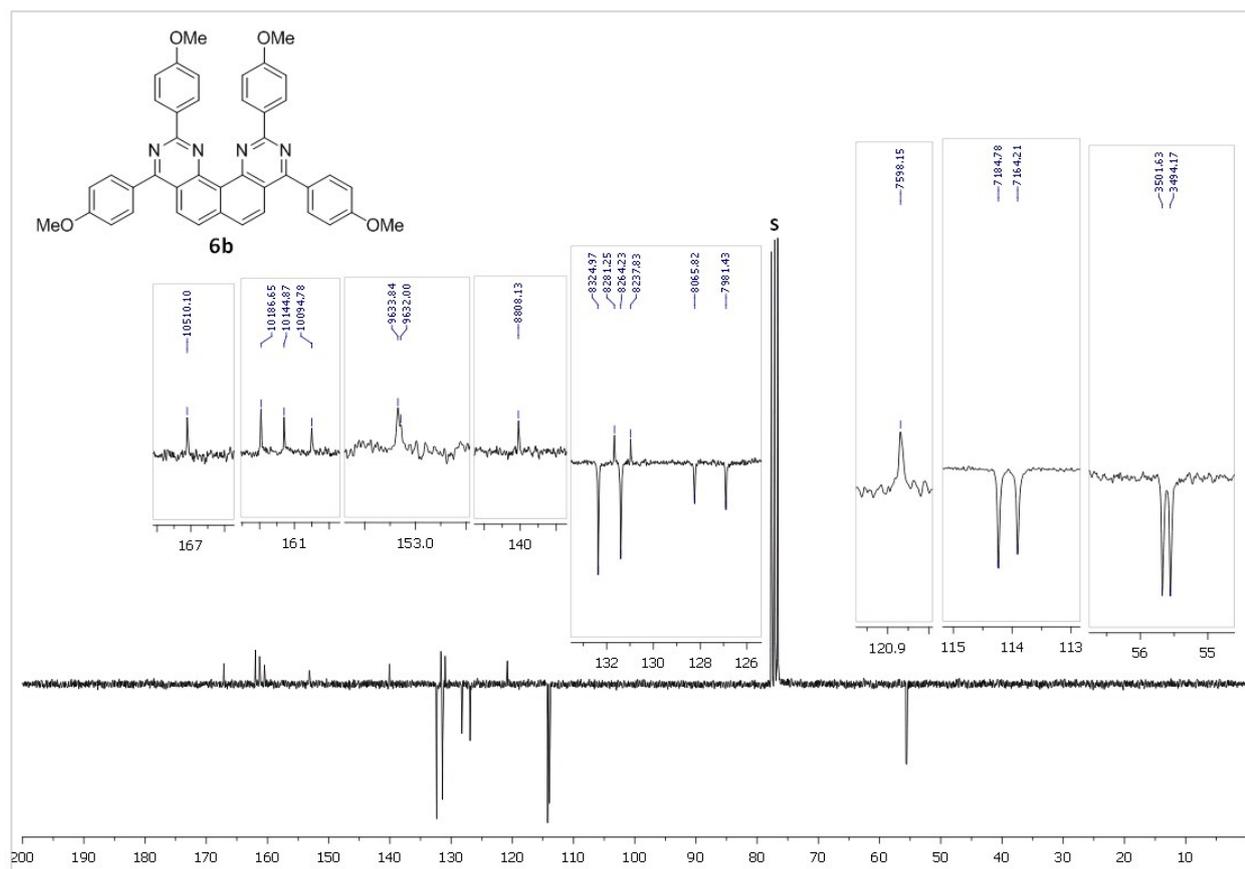
Figure S15. ^{13}C NMR spectrum of **6b** (CDCl$_3$, 63 MHz).
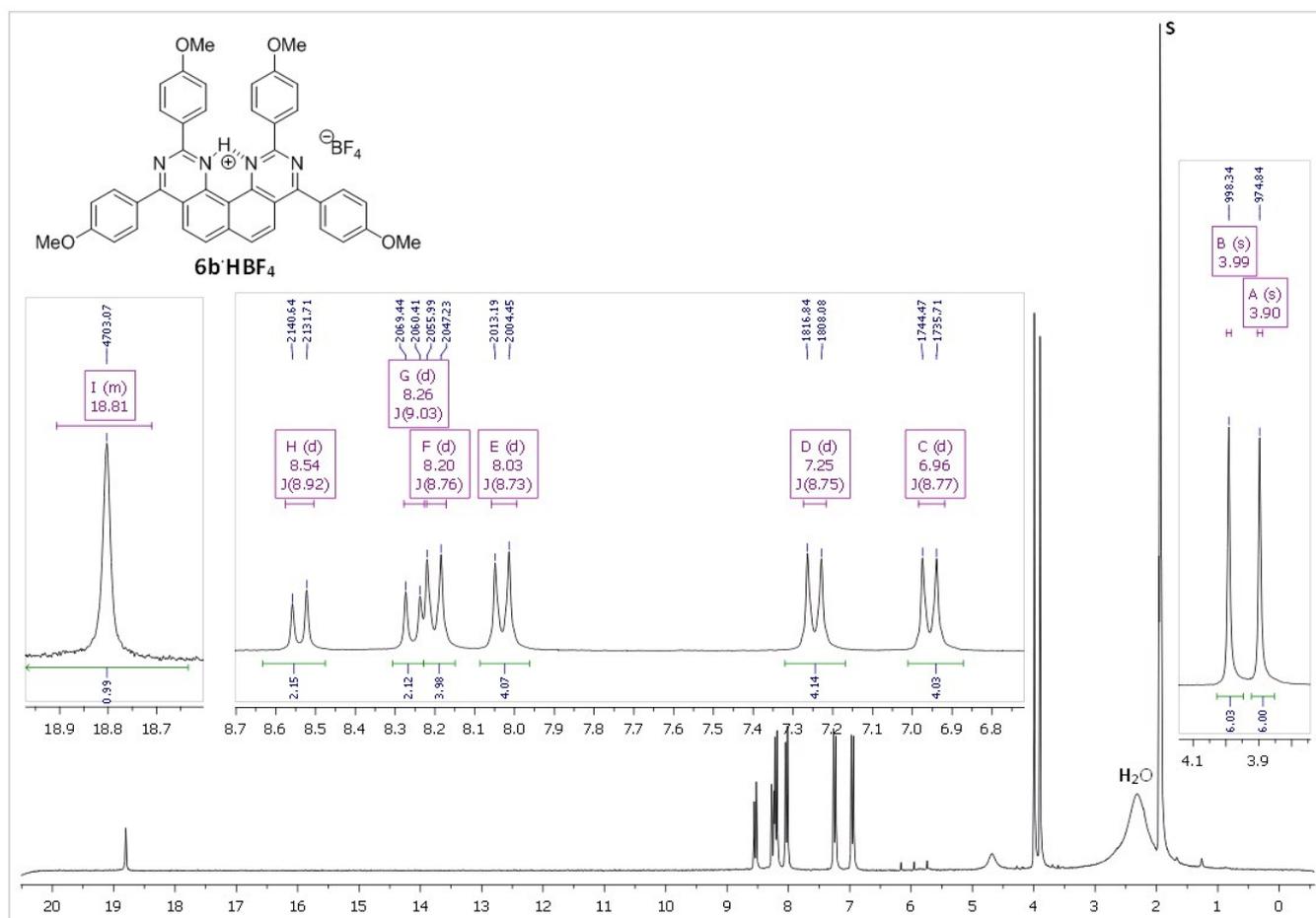
Figure S16. ^{1}H NMR spectrum of **6b·HBF$_4$** (CD$_3$CN, 250 MHz).
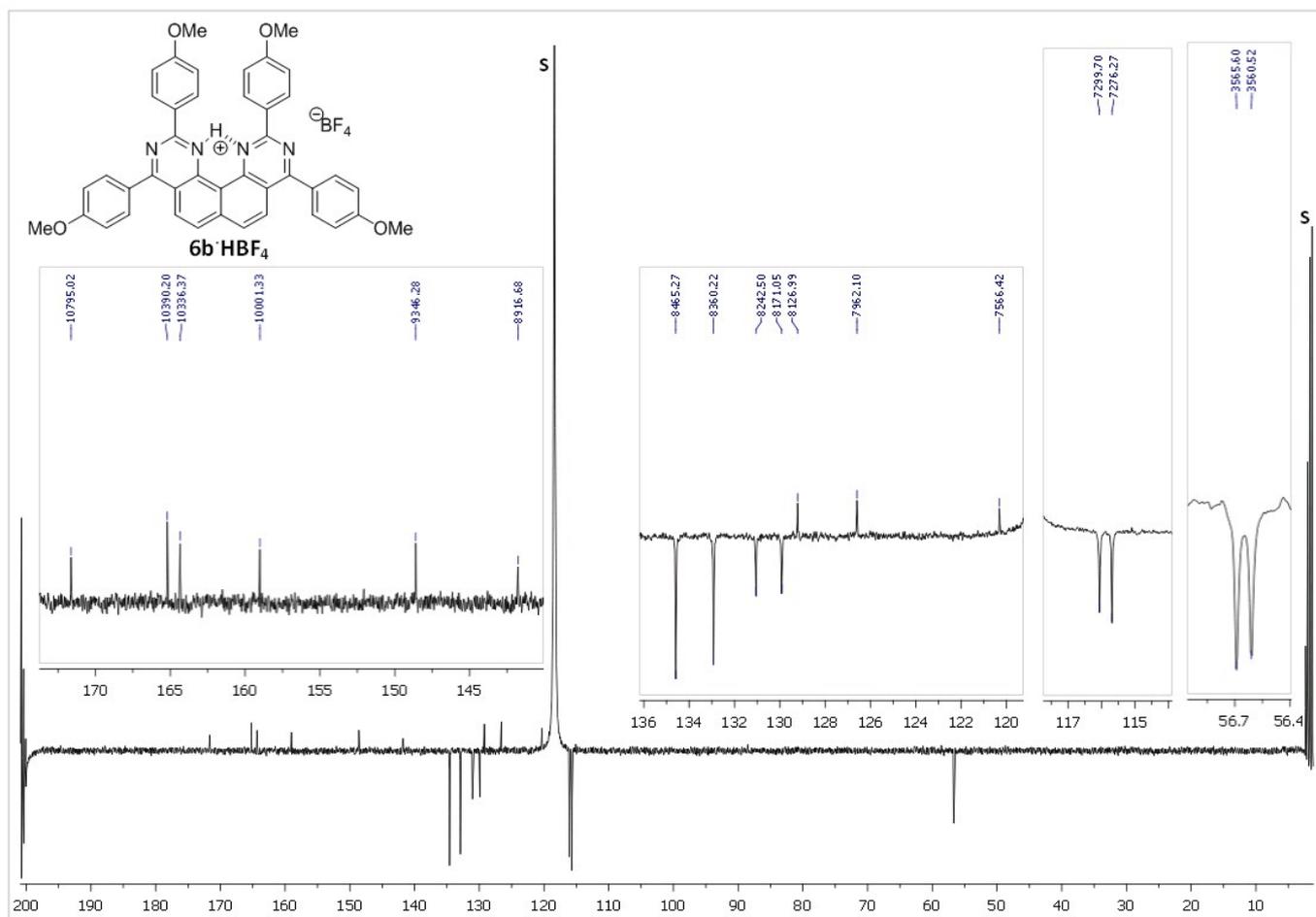
Figure S17. ^{13}C NMR spectrum of **6b·HBF$_4$** (CD$_3$CN, 63 MHz).
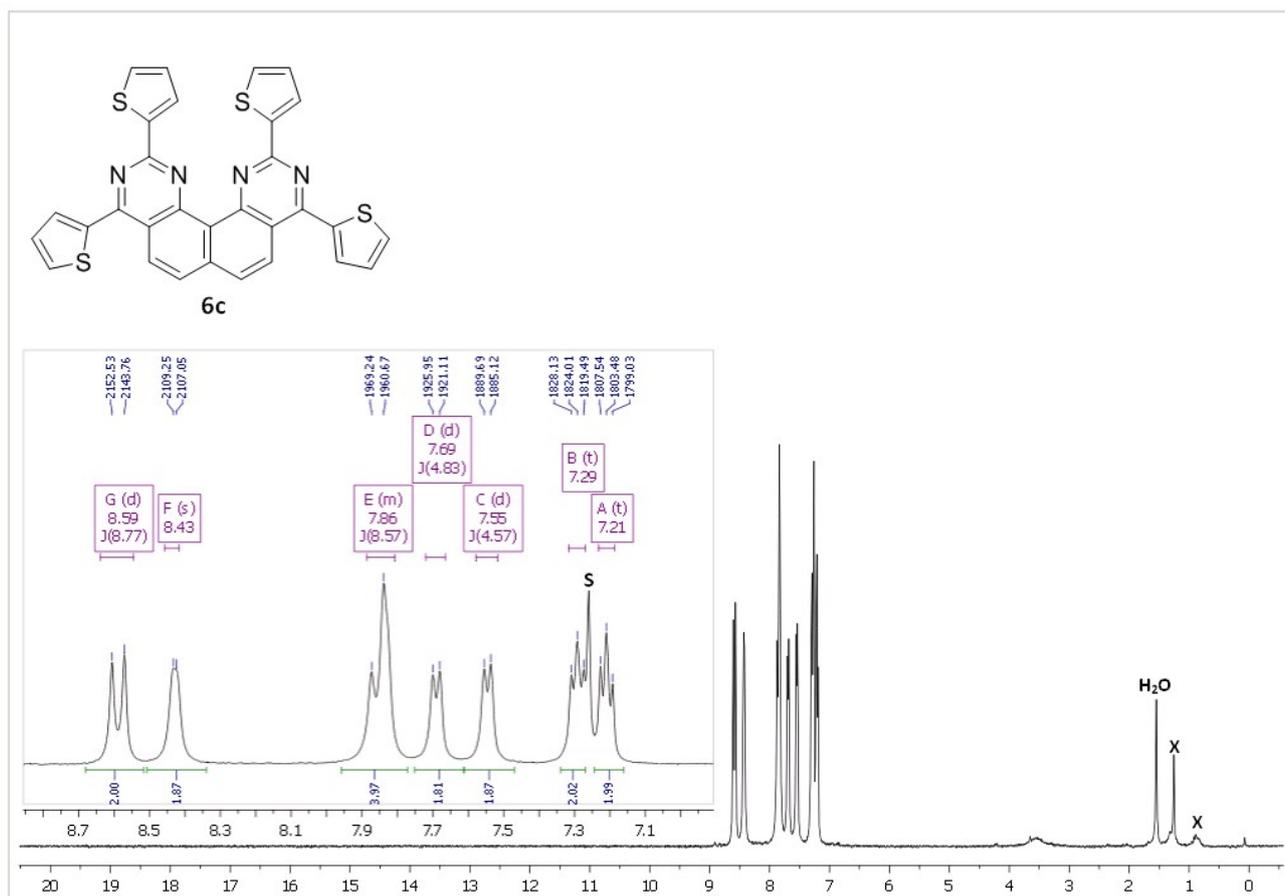
Figure S18. ^{1}H NMR spectrum of **6c** (CDCl$_3$, 250 MHz).

Figure S19. ^{13}C NMR spectrum of **6c** (CDCl$_3$, 63 MHz).

Figure S20. ^{1}H NMR spectrum of **6c·HBF$_4$** (CD$_3$CN, 250 MHz).
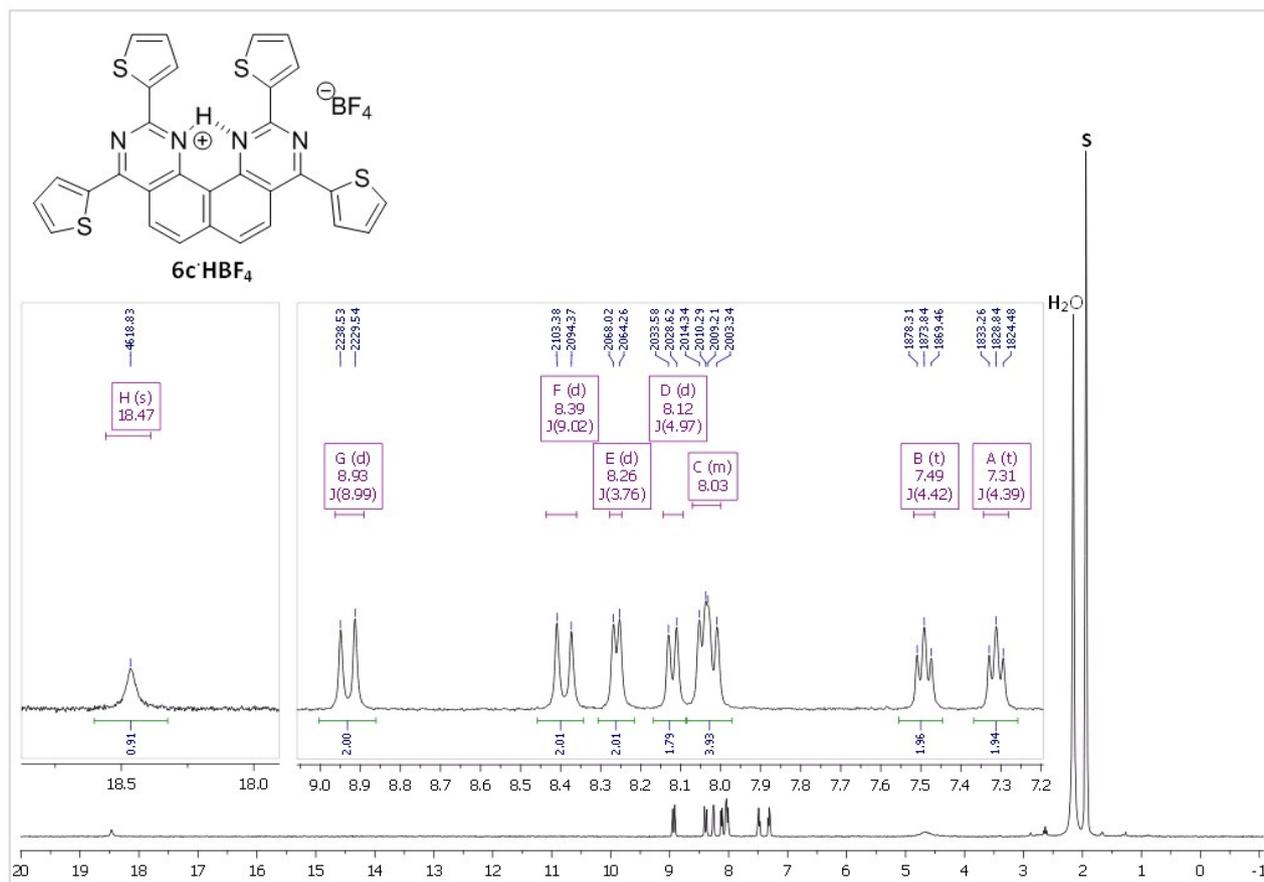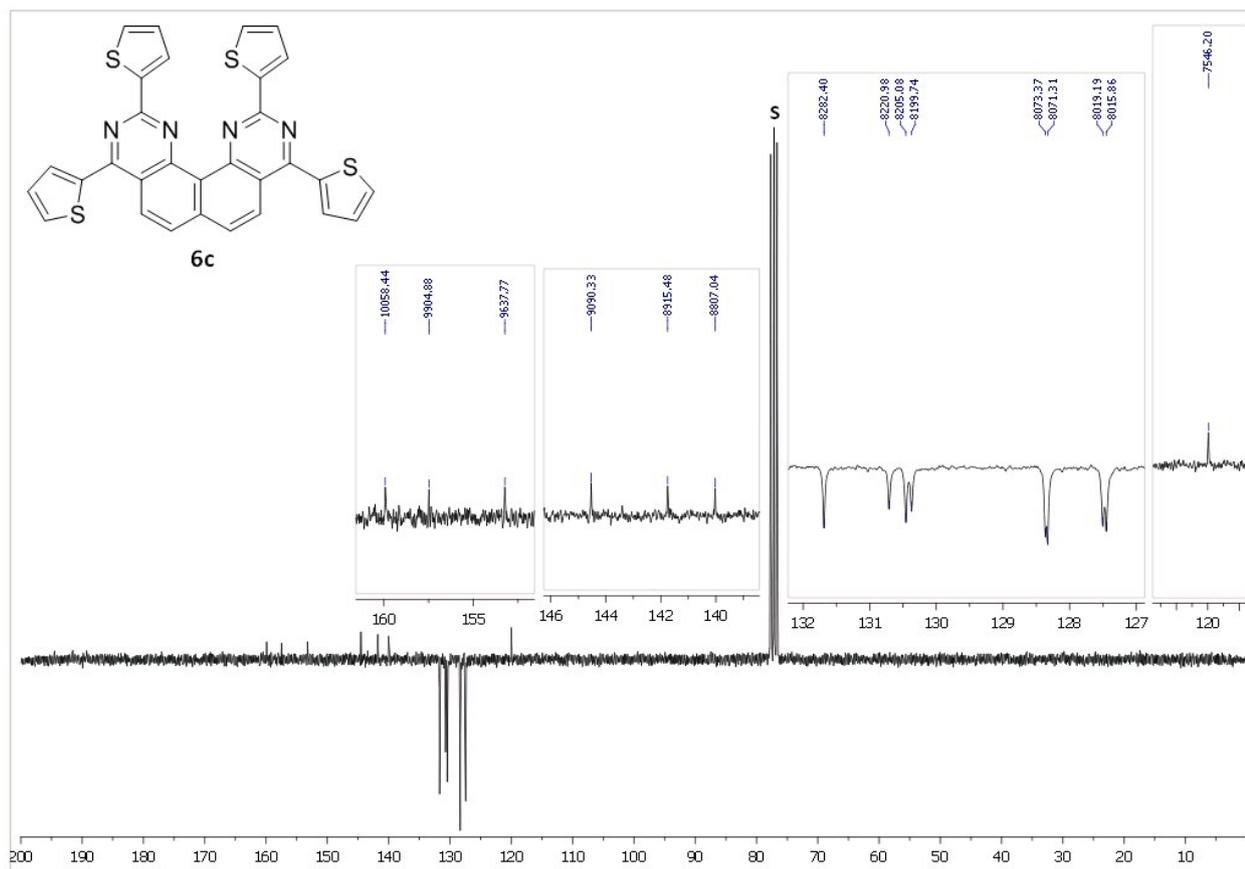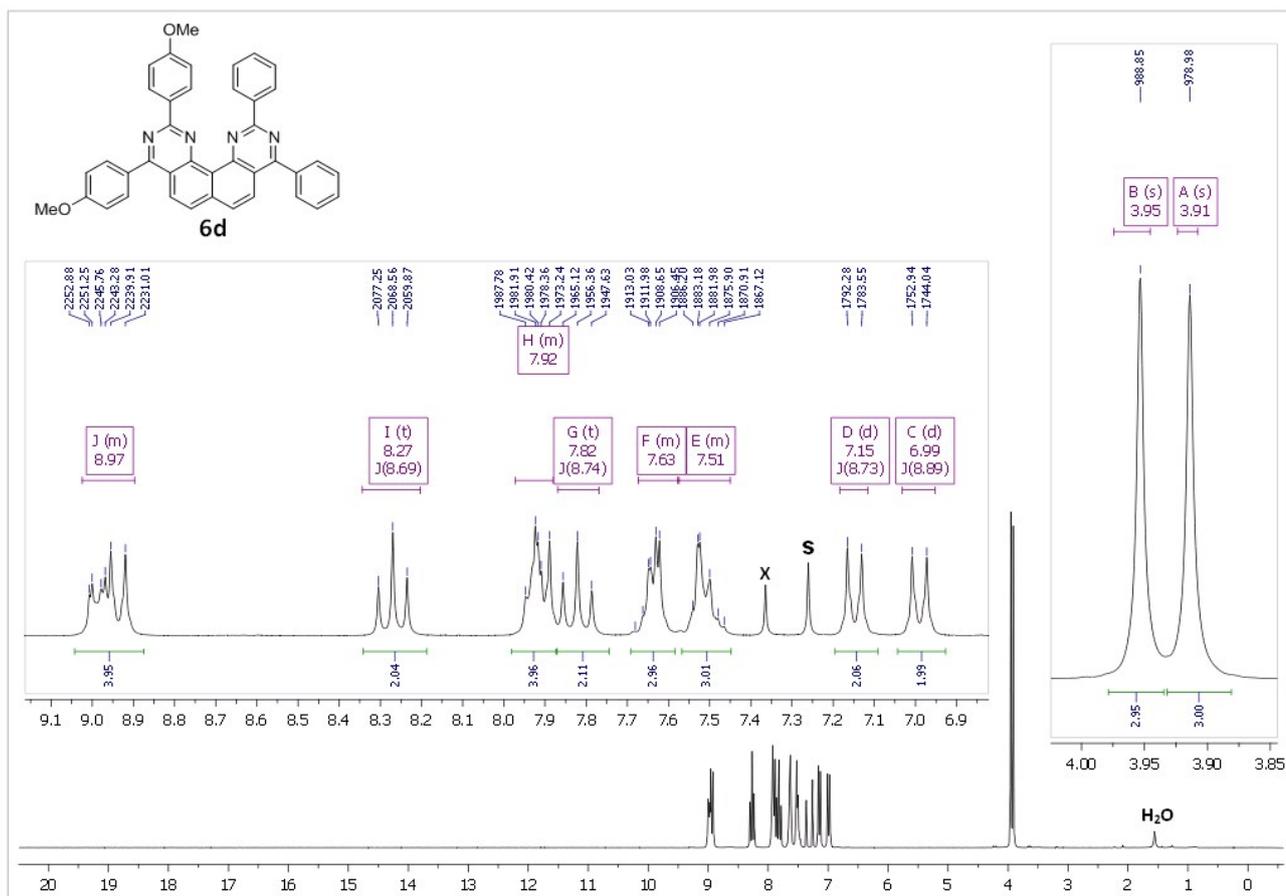
Figure S21. ^{1}H NMR spectrum of **6d** (CDCl$_3$, 250 MHz).
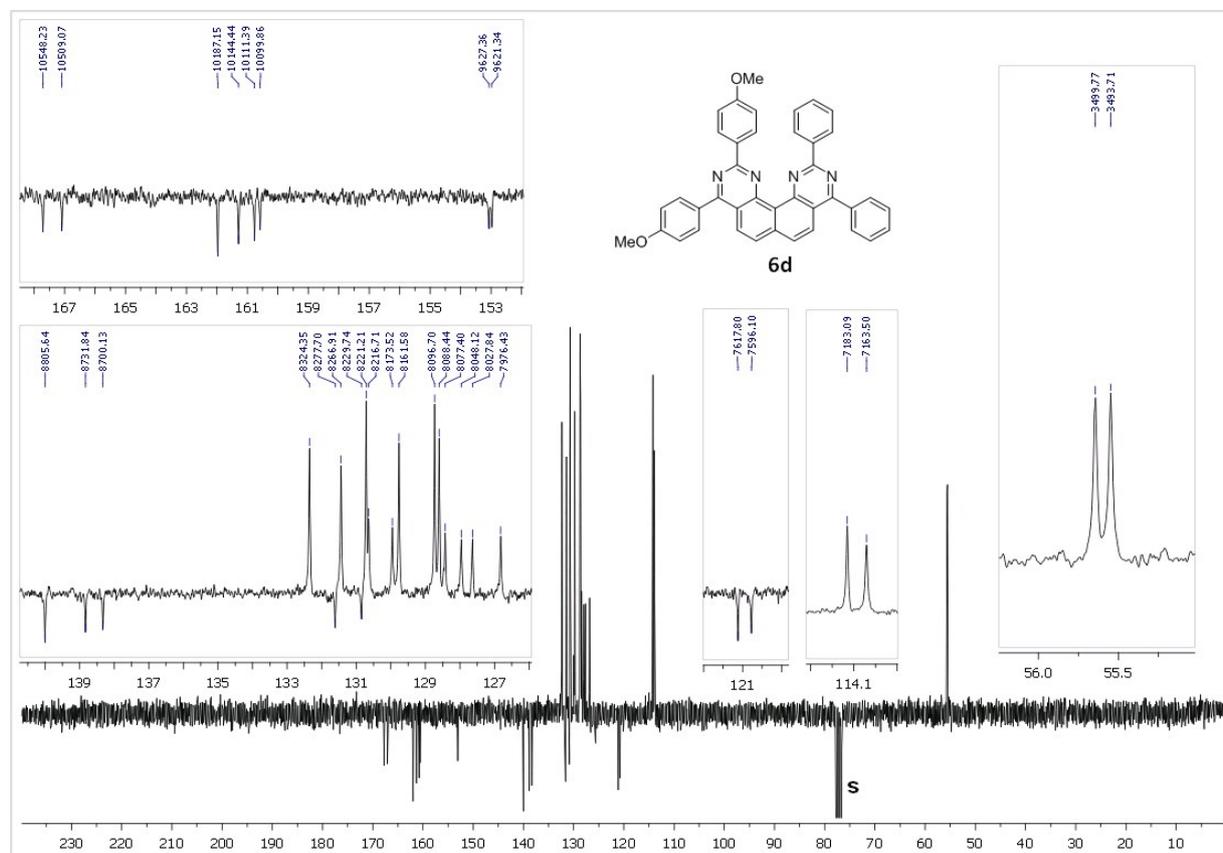
Figure S22. ^{13}C NMR spectrum of **6d** (CDCl$_3$, 63 MHz).

Figure S23. ^{1}H NMR spectrum of **6d·HBF$_4$** (CD$_3$CN, 250 MHz).

Figure S24. ^{13}C NMR spectrum of **6d·HBF$_4$** (CD$_3$CN, 63 MHz).
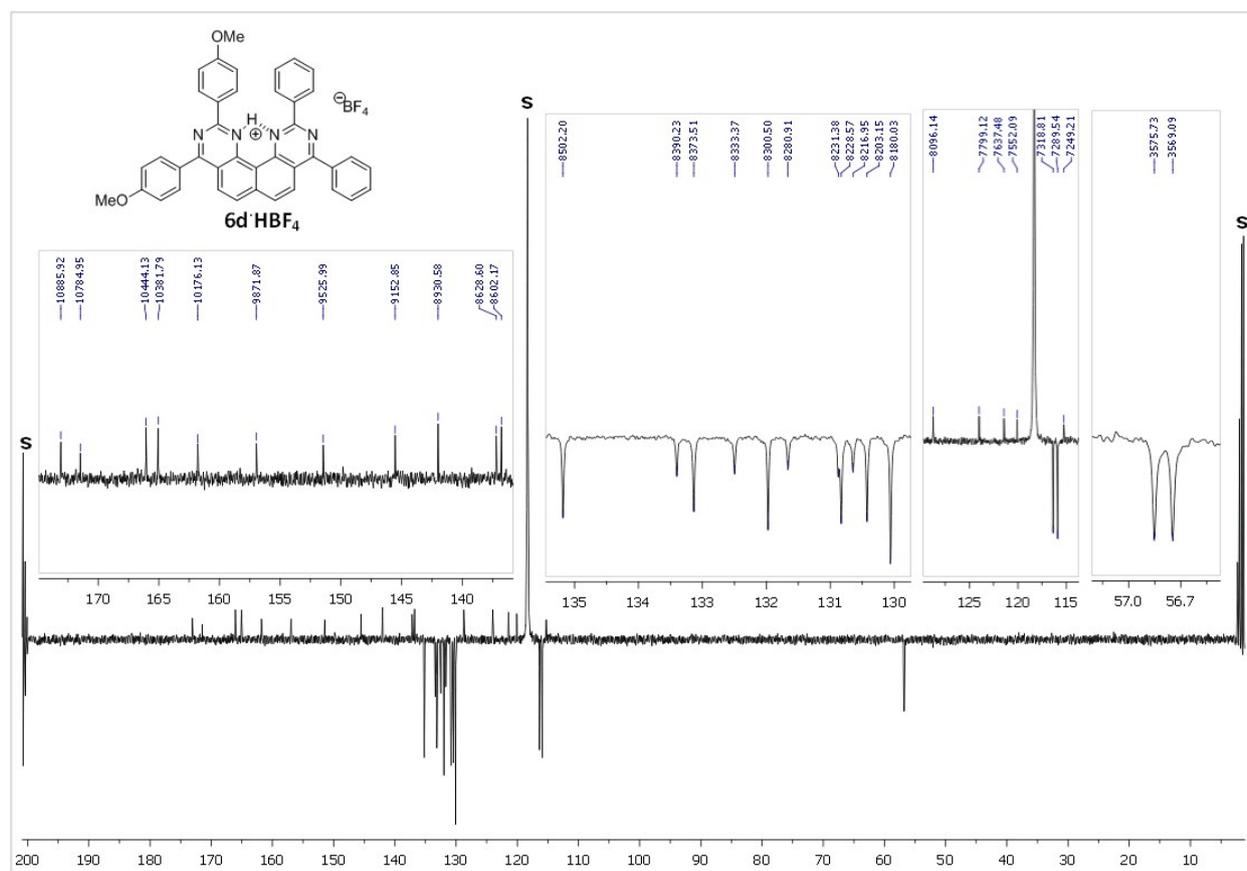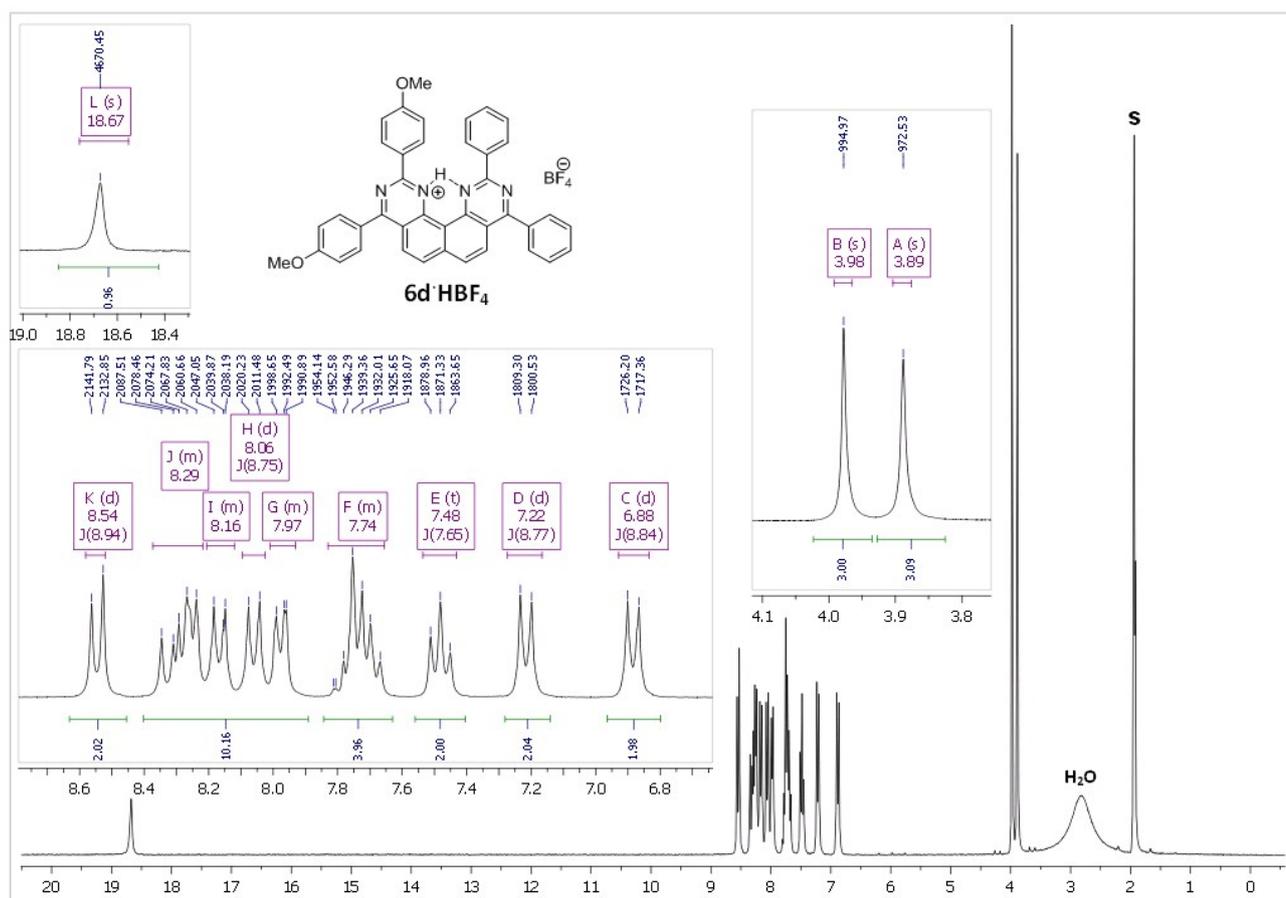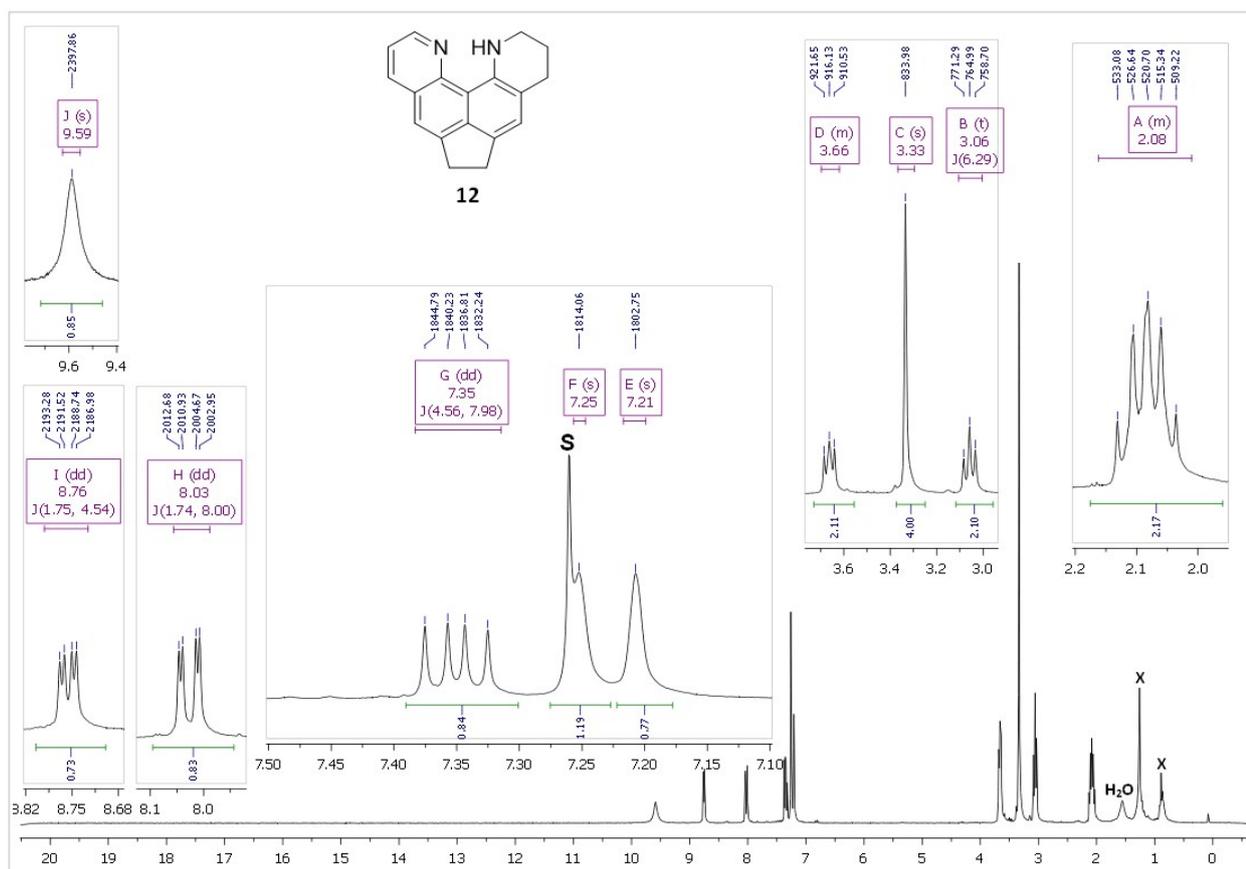
Figure S25. ^{1}H NMR spectrum of **12** (CDCl$_3$, 250 MHz).
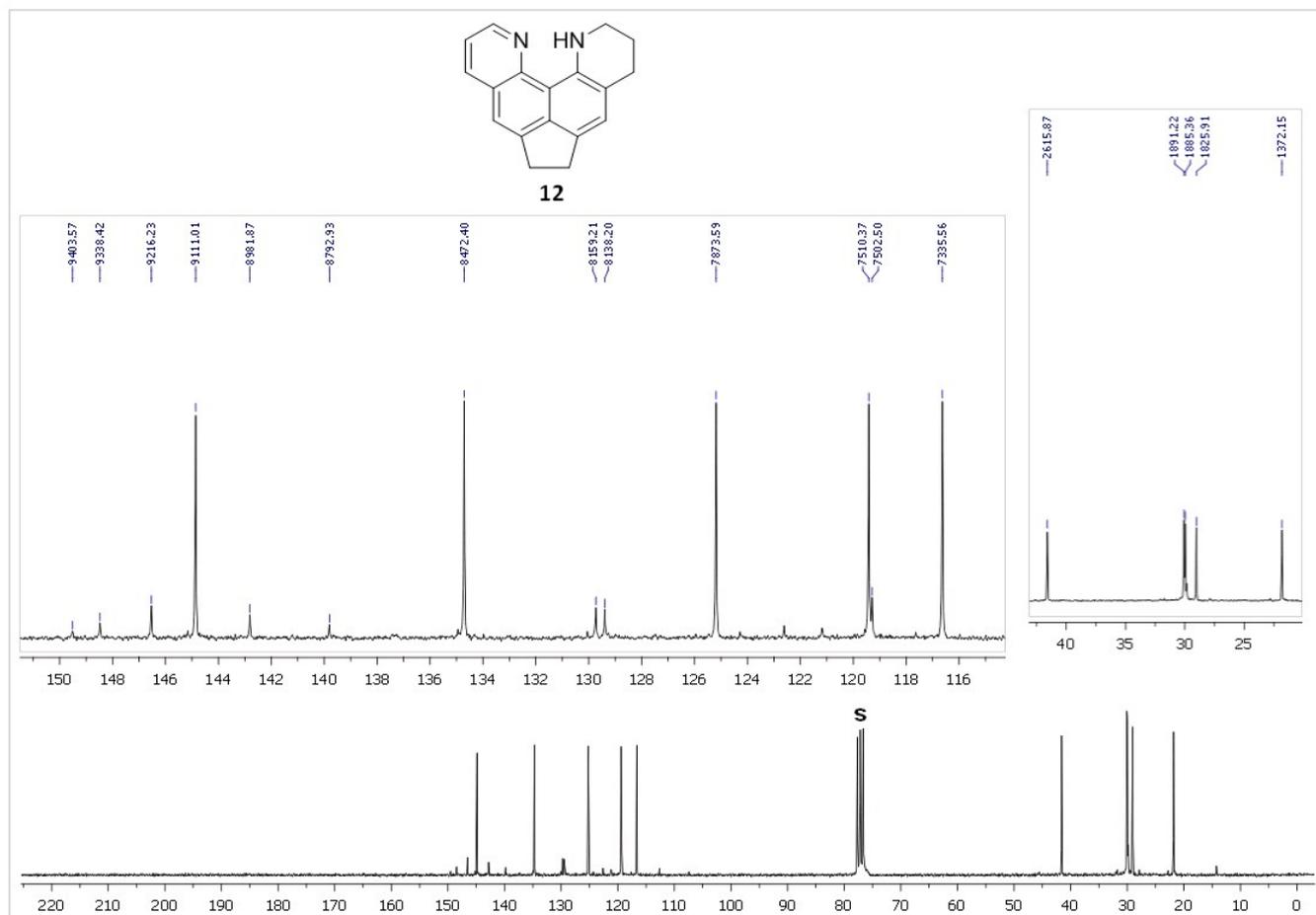
Figure S26. ^{13}C NMR spectrum of **12** (CDCl$_3$, 63 MHz).
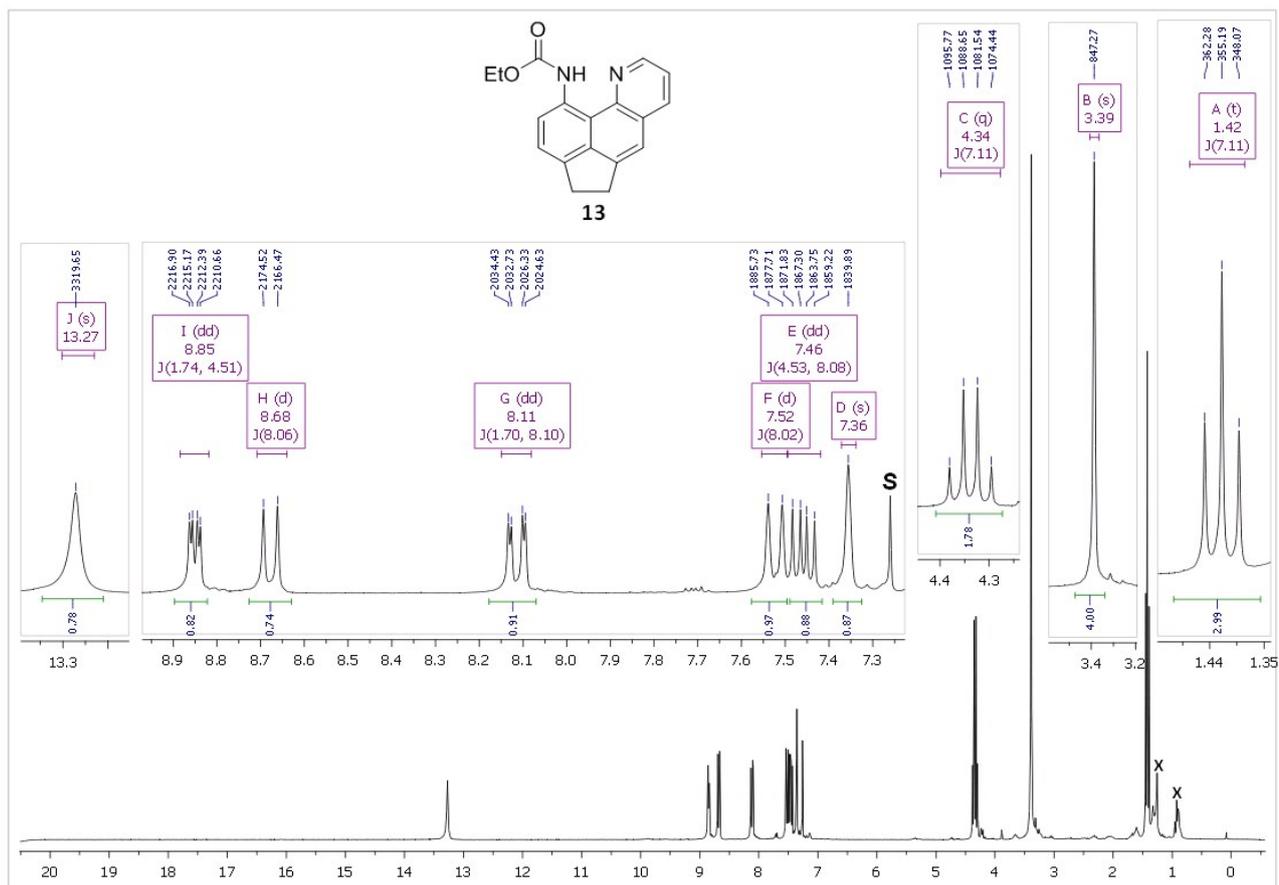
Figure S27. ^{1}H NMR spectrum of **13** (CDCl$_3$, 250 MHz).
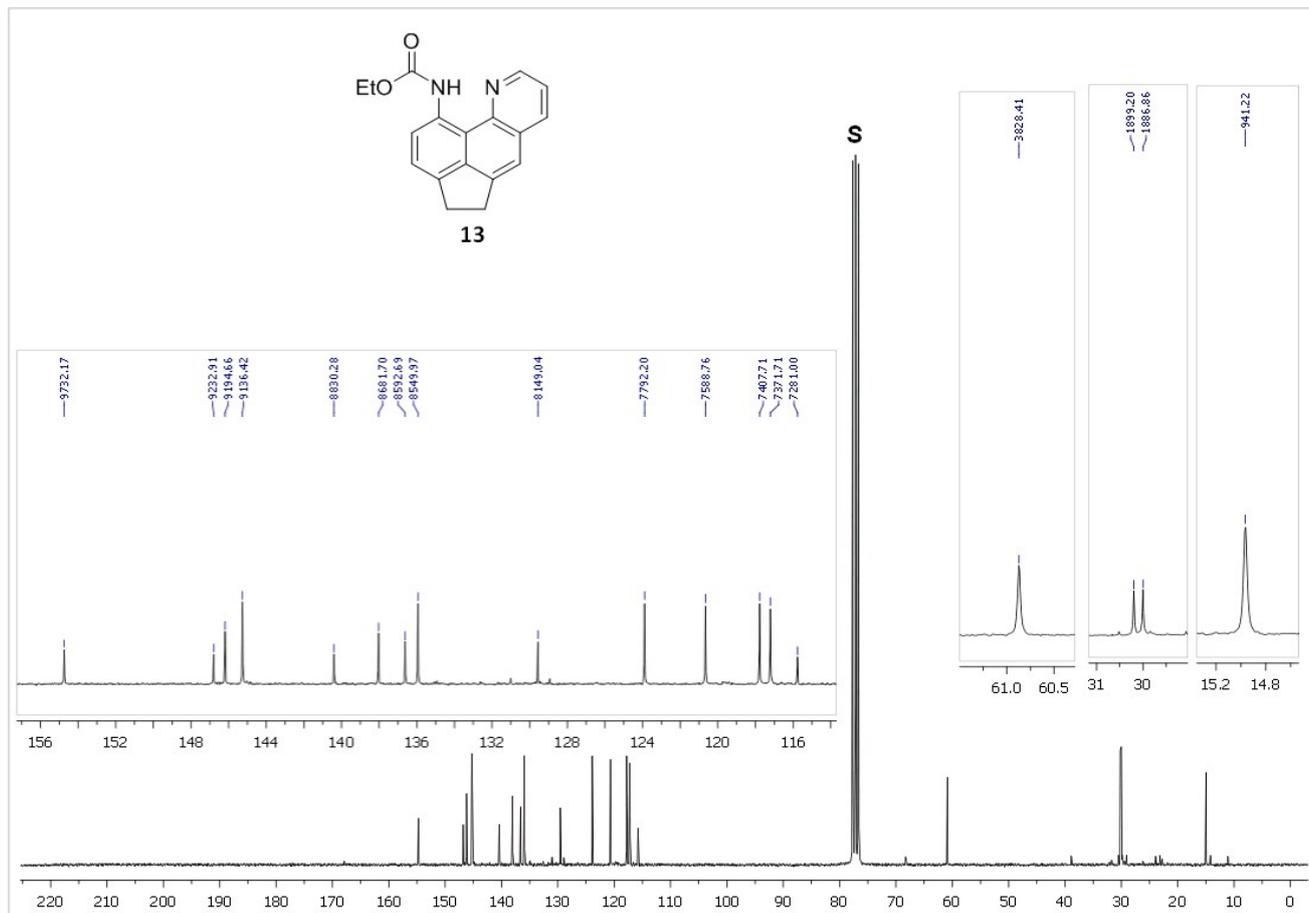
Figure S28. ^{13}C NMR spectrum of **13** (CDCl$_3$, 63 MHz).

Gas-phase proton affinities, PA, for **6a** and **3** (R = Ph) (B3LYP/6-311++G**).
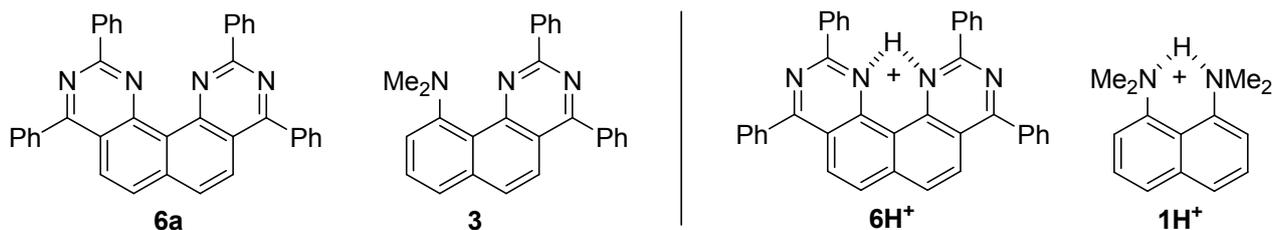
They are equal to 261.65 and 256.62 kcal/mol, respectively (252.93 and 248.16 kcal/mol with ZPE correction). At first glance, these values may seem improbable, since they mean a greater basicity of **6** than the proton sponge **1** (253.40 and 244.79 kcal/mol with ZPE correction). However, one should not forget that in vacuum, i.e. in the absence of solvation, the acid-base properties are strongly influenced by the size of the cation or anion: larger ions, such as **6H$^+$** in comparison with **1H$^+$**, are better stabilized due to more efficient charge dispersion.

Table S1. Selected Absorption and Emission Parameters of the Studied Compounds (in MeCN)

Compd.	Absorption λ_{max}, nm ($\varepsilon \cdot 10^{-3}$ M^{-1}cm^{-1})*	Emission, λ_{max}, nm	Stokes shift, nm (cm^{-1})	Quantum yield
5	378 (14.96) 359 (9.68) 341 (4.15) 318 (4.59) 306 (8.43) 273 (46.29) 245 (25.08) 221 (29.51)	-	-	-
5·HClO₄	395 (12.95) 374 (9.38) 351 (6.22) 269 (35.48) 243 (28.13) 231 (28.58) 218 (26.71)	426 (427)**	31 (1840)	0.711 (0.299)**
6a	400, 380, 329, 292, 258	-	-	-
6b	415 (15.36) 394 (12.32) 309 (38.80) 271 (32.43) 258 (36.32)	-	-	-
6c	433, 409, 320 274, 226	-	-	-
6d	409, 389, 307 291, 268, 253	-	-	-
6a·HBF₄	430 (22.89) 407 (17.54) 304 (44.76) 255 (44.35)	486	56 (1744)	0.773
6b·HBF₄	456 (21.40) 432 (15.86) 383 (19.99) 320 (24.40) 289 (22.70) 265 (29.39) 220 (28.30)	558	102 (2167)	0.018
6c·HBF₄	475 (35.12) 448 (25.25) 382 (24.30) 351 (34.70) 326 (36.56) 273 (34.00) 222 (28.65)	555	80 (2042)	0.185
6d·HBF₄	446 (33.37) 421 (25.80) 391 (24.62) 303 (34.74) 263 (46.15)	593	147 (2028)	0.007

*Due to low solubility exact values of extinction for bases **6a**, **6c** and **6d** could not be measured.
** The values found in water are given in parentheses.
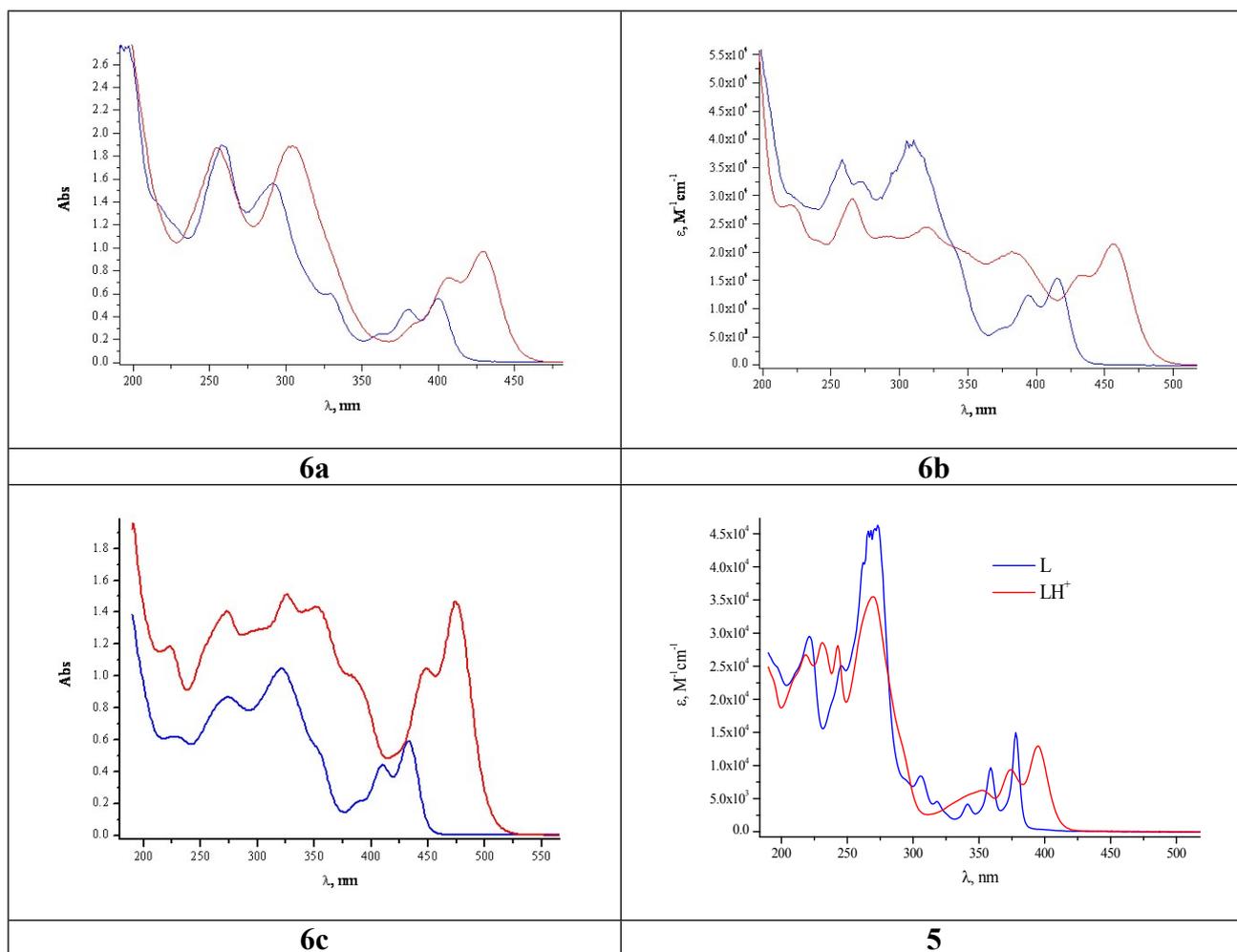
Figure S29. Absorption spectra of compounds **5** and **6a–c** (blue) and their salts **5H⁺ClO₄⁻** and **6H⁺BF₄⁻** (red) in MeCN.
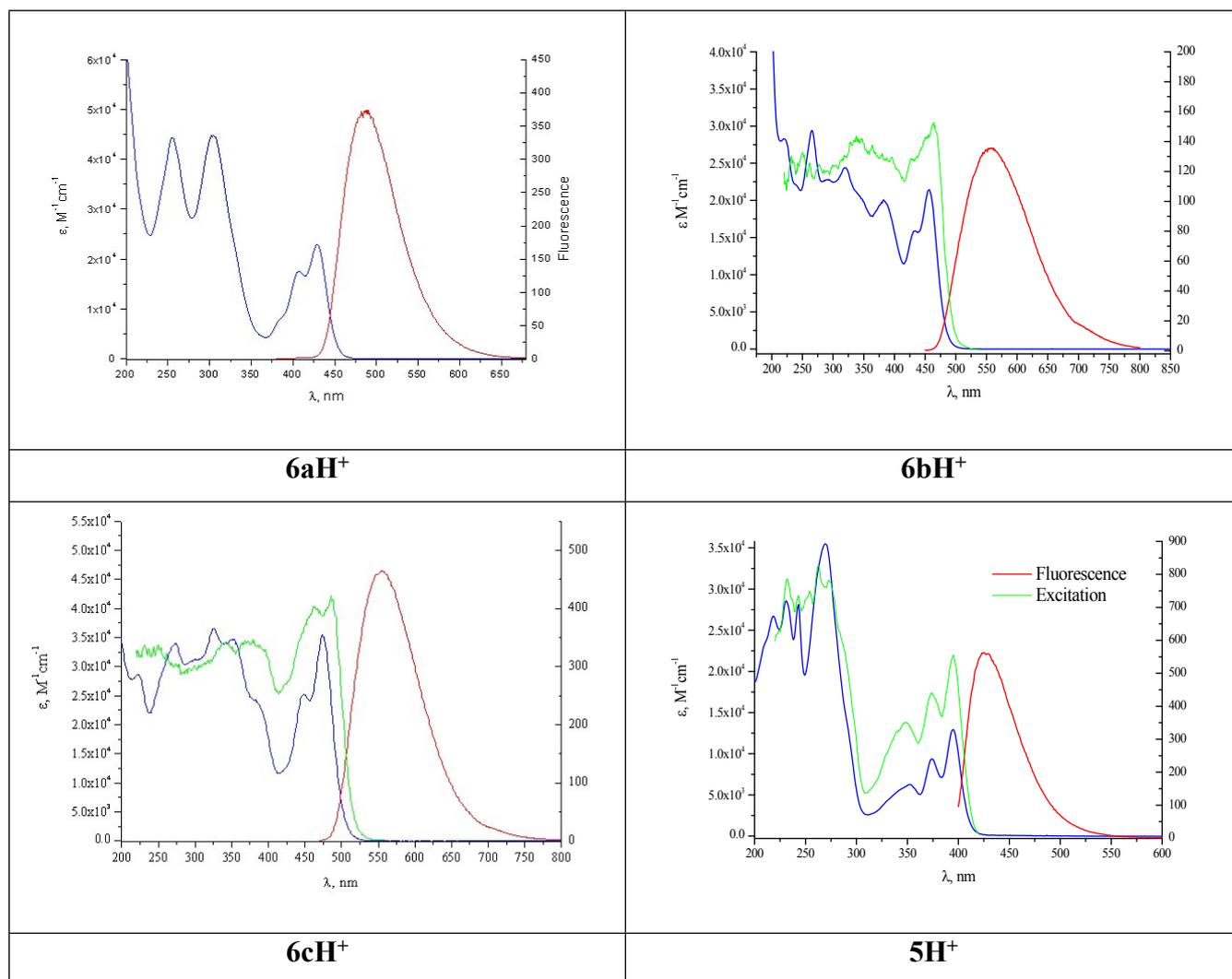
Figure S30. Absorption (blue), excitation (green) and emission (red) spectra for salts **6a–c·HBF₄** and **5·HClO₄** in MeCN.
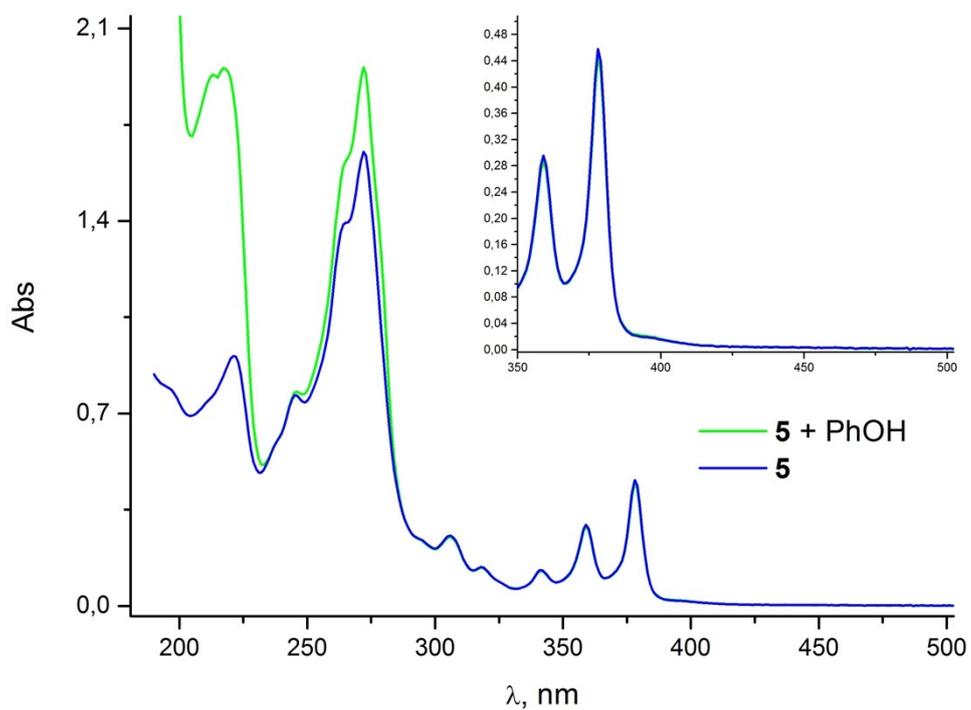
Figure S31. Absorption spectrum of base **5** in acetonitrile in the absence and in the presence of phenol, $c(\mathbf{5}) = 3.47 \cdot 10^{-5}$ M, $c(\text{PhOH}) = 2.4 \cdot 10^{-4}$ M.
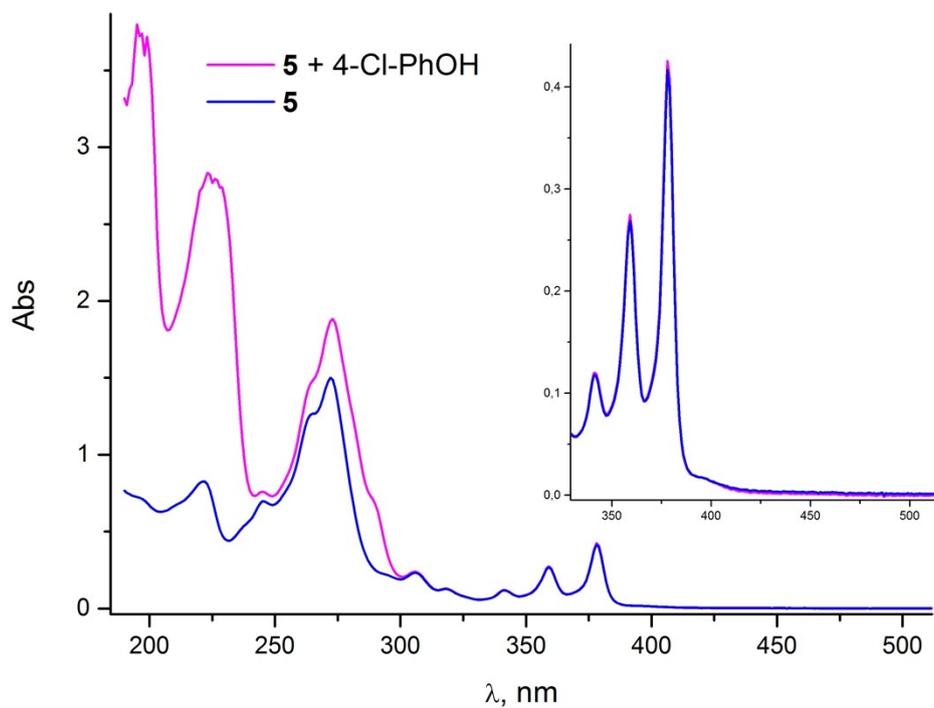
Figure S32. Absorption spectrum of base **5** in acetonitrile in the absence and in the presence of 4-chlorophenol, $c(\mathbf{5}) = 3.47 \cdot 10^{-5}$ M, $c(\text{4-Cl-C}_6\text{H}_4\text{OH}) = 2.9 \cdot 10^{-4}$ M.
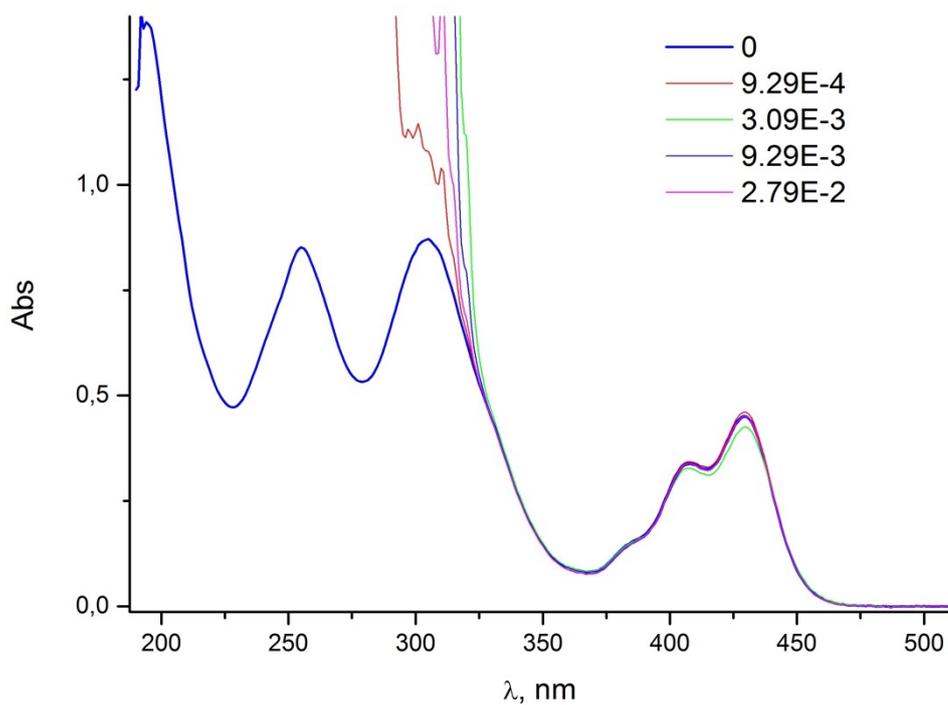
Figure S33. Absorption spectra of salt **6aH⁺ClO₄⁻** in acetonitrile ($c = 2 \cdot 10^{-5}$ M) in the presence of naphthalene. The concentrations of naphthalene are presented on the panel.
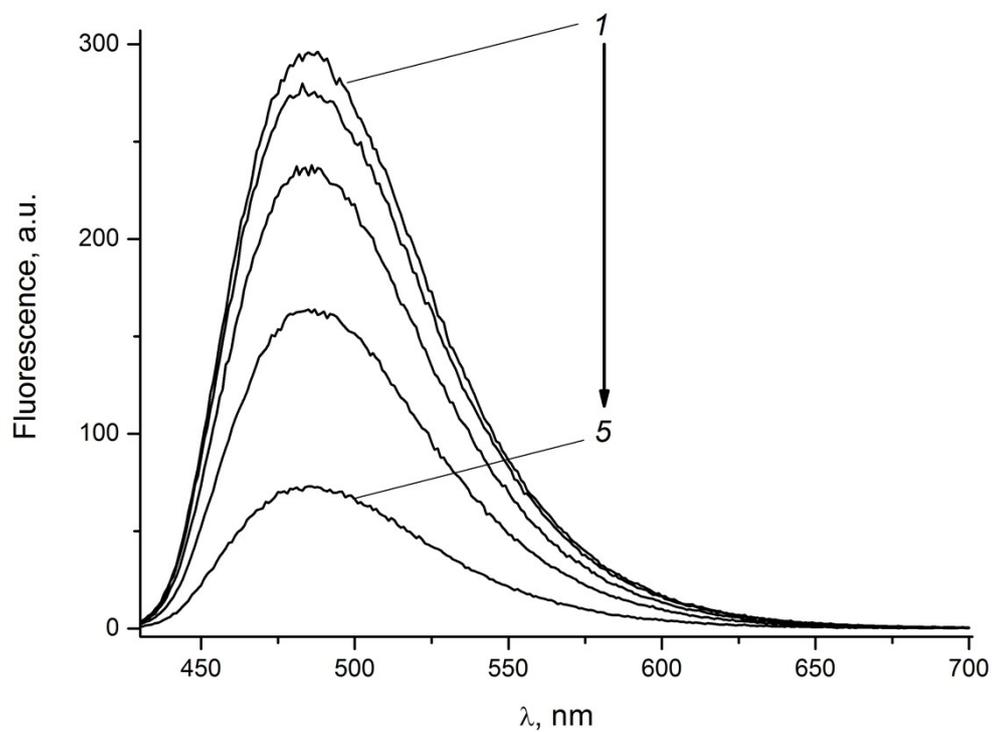
**Figure S34.** Fluorescence emission spectra of salt **6aH⁺ClO₄⁻** in acetonitrile ($c = 2 \cdot 10^{-5}$ M) in the presence of naphthalene. The concentrations of naphthalene: *1* – 0, *2* – $9.29 \cdot 10^{-4}$ M, *3* – $3.09 \cdot 10^{-3}$ M, *4* – $9.29 \cdot 10^{-3}$ M, *5* – $2.79 \cdot 10^{-2}$ M.
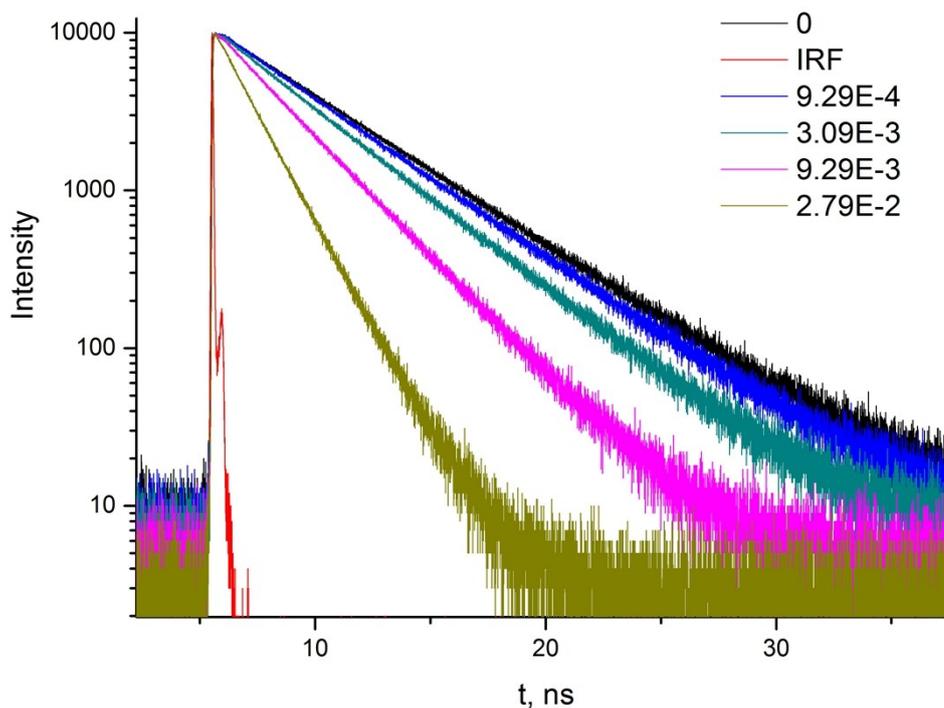
Figure S35. Fluorescence decay of salt **6aH⁺ClO₄⁻** in acetonitrile (c = 2·10⁻⁵ M) in the presence of naphthalene. The concentrations of naphthalene are presented on the panel.
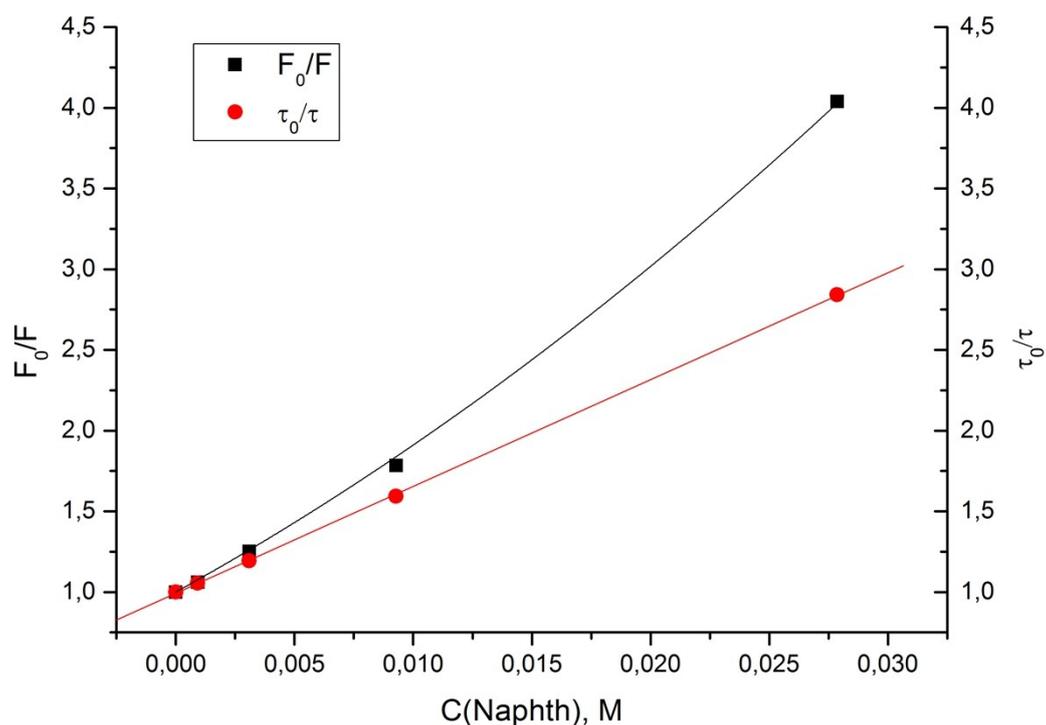
Figure S36. Fluorescence intensity (black squares) and lifetime (red circles) Stern-Volmer plots of **6aH⁺ClO₄⁻** quenching by naphthalene in MeCN. All lifetime values were measured at 480 nm. Symbols correspond to experimental data, lines are fittings according eq. 1 (τ_0/τ) and eq. 2 (F_0/F).
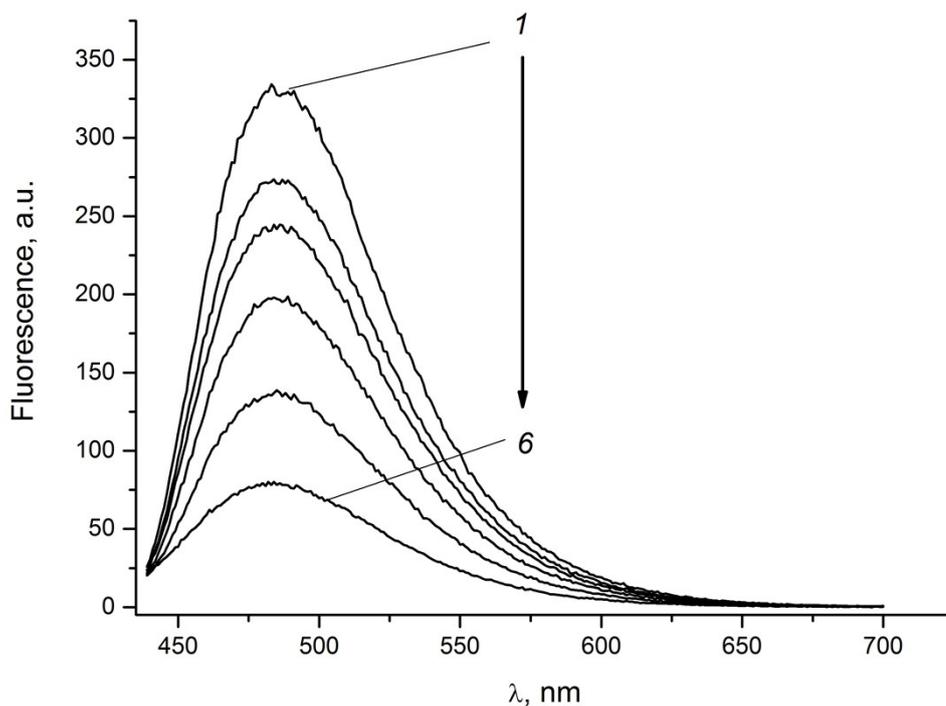
Figure S37. Fluorescence emission spectra of salt $6aH^+ClO_4^-$ in acetonitrile ($c = 2 \cdot 10^{-5}$ M) in the presence of indole. The concentrations of indole: $1 - 0$, $2 - 5.32 \cdot 10^{-4}$ M, $3 - 1.77 \cdot 10^{-3}$ M, $4 - 3.55 \cdot 10^{-3}$ M, $5 - 7.09 \cdot 10^{-3}$ M, $6 - 1.42 \cdot 10^{-2}$ M.
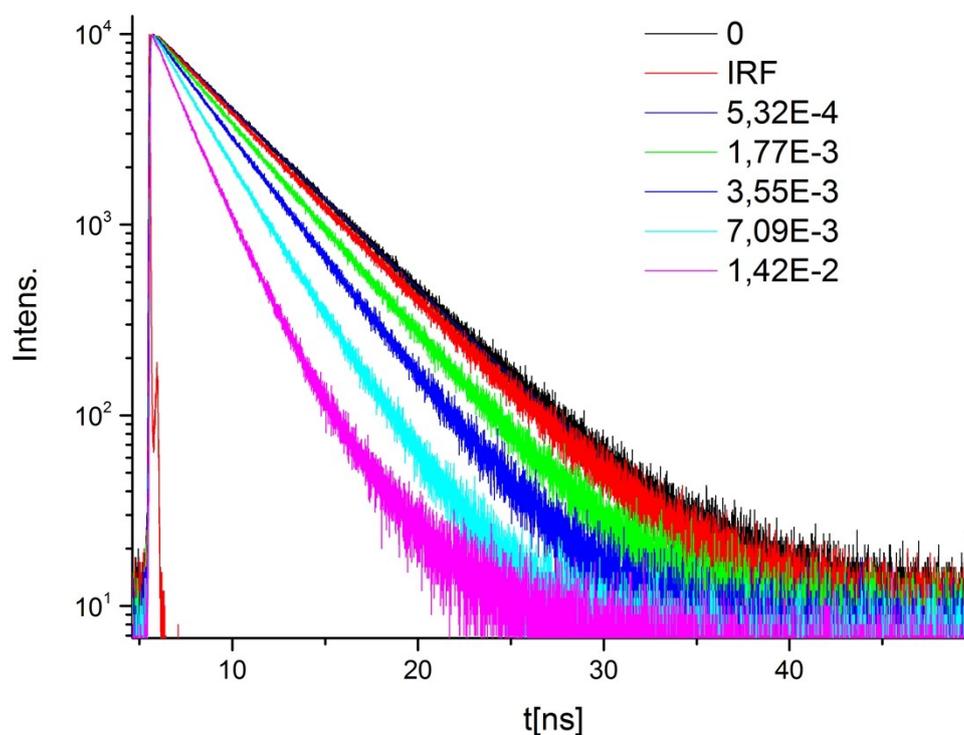

Figure S38. Fluorescence decay of salt $6aH^+ClO_4^-$ in acetonitrile ($c = 2 \cdot 10^{-5}$ M) in the presence of indole. The concentrations of indole are presented on the panel.
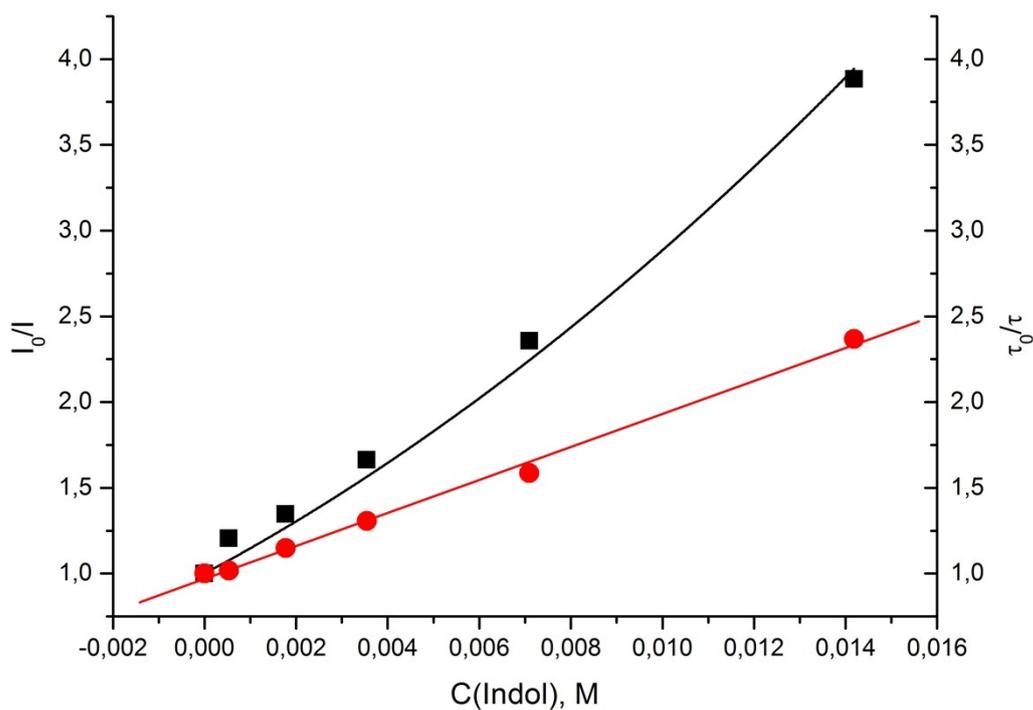
Figure S39. Fluorescence intensity (black squares) and lifetime (red circles) Stern-Volmer plots of **6aH⁺ClO₄⁻** quenching by indole in MeCN. All lifetime values were measured at 480 nm. Symbols correspond to experimental data, lines are fittings according eq. 1 (τ_0/τ) and eq. 2 (I_0/I).
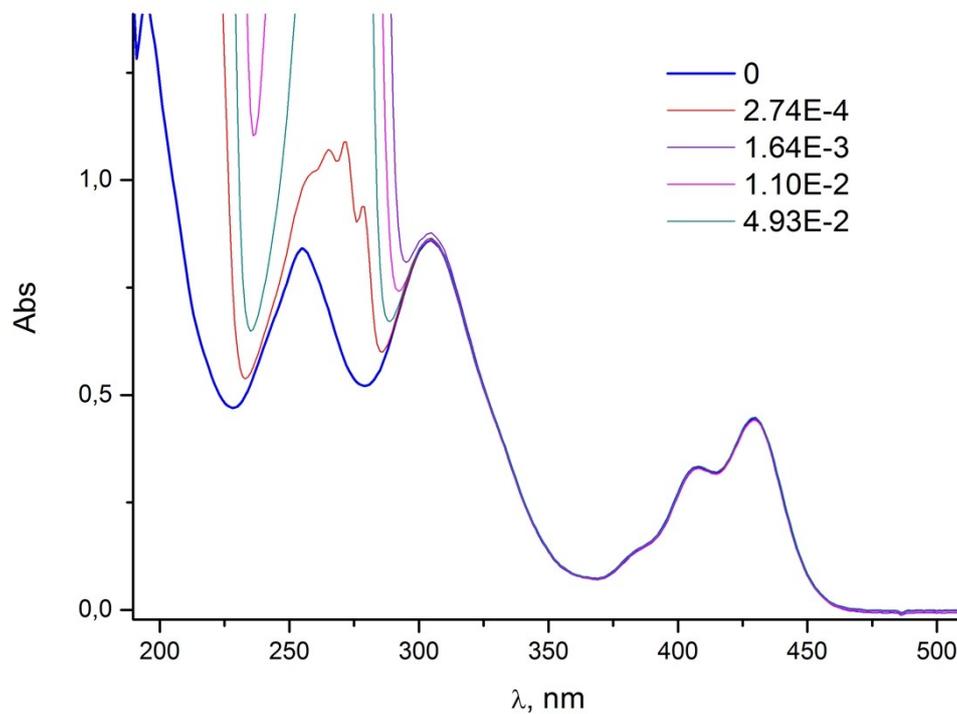
Figure S40. Absorption spectra of salt **6aH⁺ClO₄⁻** in acetonitrile ($c = 2 \cdot 10^{-5}$ M) in the presence of PhOH. The concentrations of PhOH are presented on the panel.
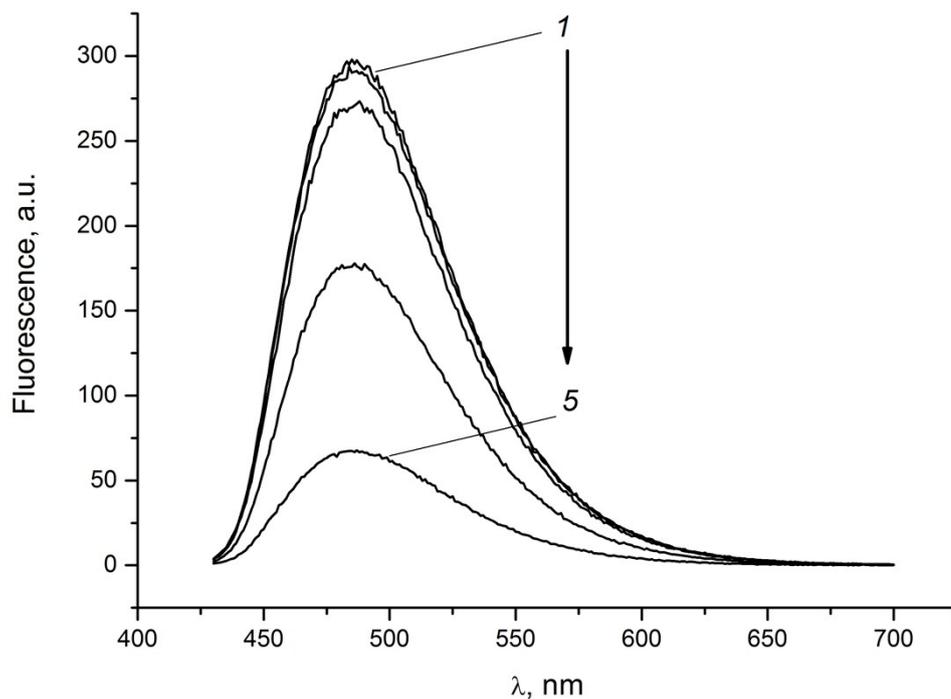
Figure S41. Fluorescence emission spectra of salt **6aH⁺ClO₄⁻** in acetonitrile in the presence of PhOH. The concentrations of PhOH: *1* – 0, *2* – 2.74·10⁻⁴ M, 3 – 1.64·10⁻³ M, *4* – 1.10·10⁻² M, *5* – 4.93·10⁻² M.
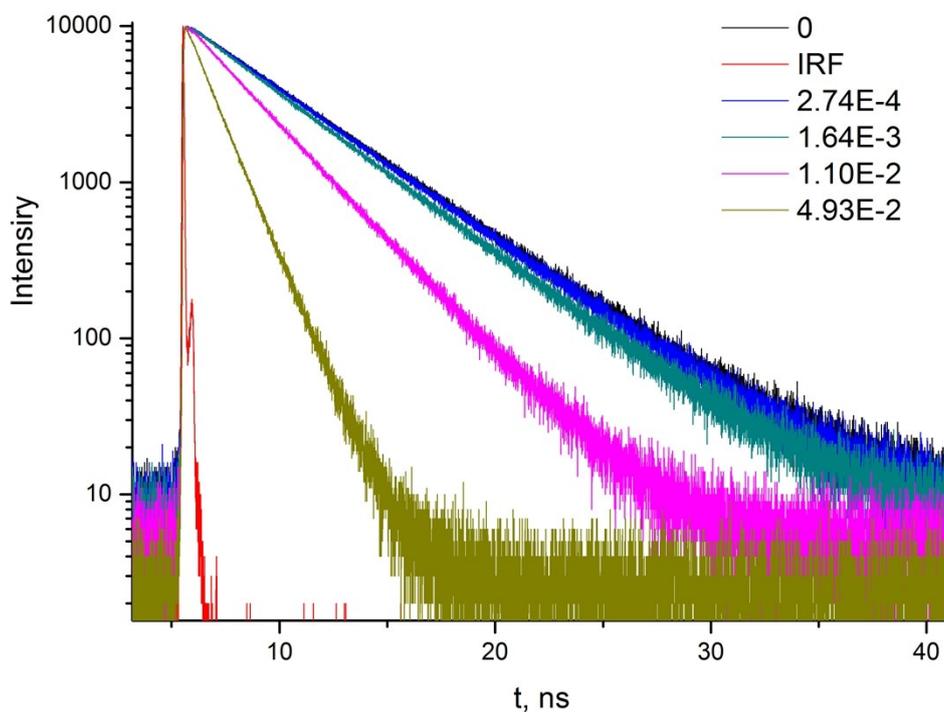
Figure S42. Fluorescence decay of salt **6aH⁺ClO₄⁻** in acetonitrile (*c* = 2·10⁻⁵ M) in the presence of PhOH. The concentrations of PhOH are presented on the panel.
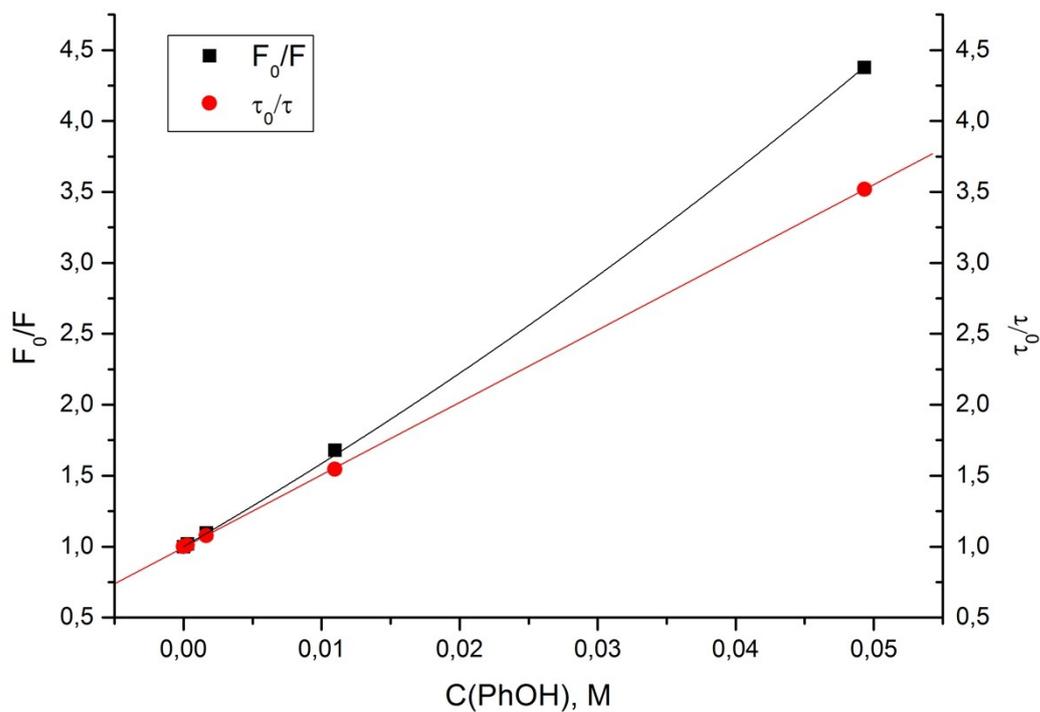
Figure S43. Fluorescence intensity (black squares) and lifetime (red circles) Stern-Volmer plots of **6aH⁺ClO₄⁻** quenching by PhOH in MeCN. All lifetime values were measured at 480 nm. Symbols correspond to experimental data, lines are fittings according eq. 1 (τ_0/τ) and eq. 2 (F_0/F).
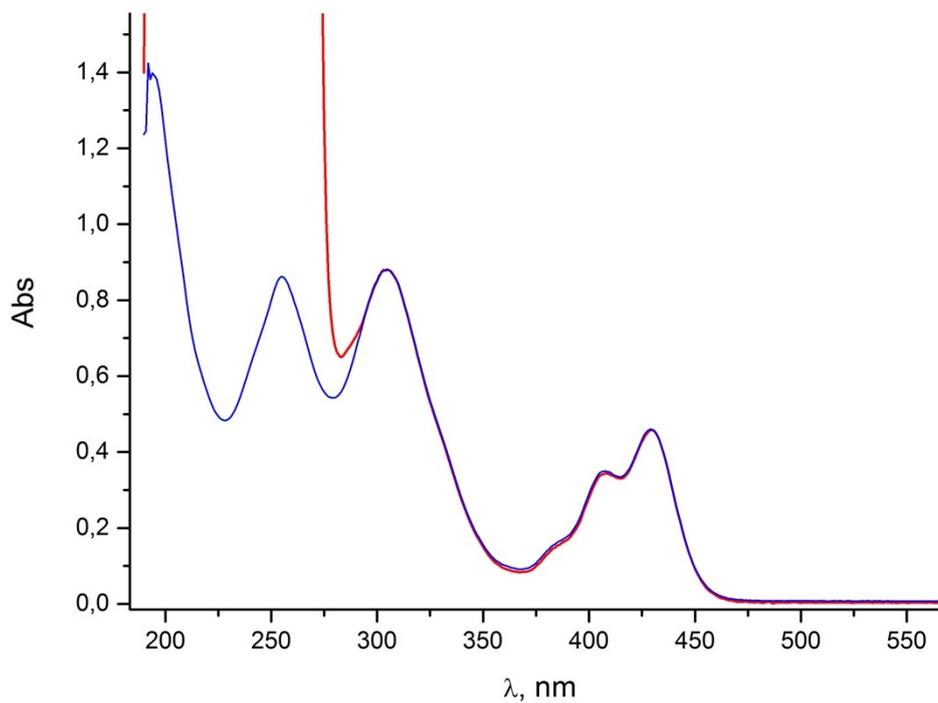

Figure S44. Absorption spectra of salt **6aH⁺ClO₄⁻** in acetonitrile ($c = 2 \cdot 10^{-5}$ M) in the presence of 100 eq. PhCF₃.
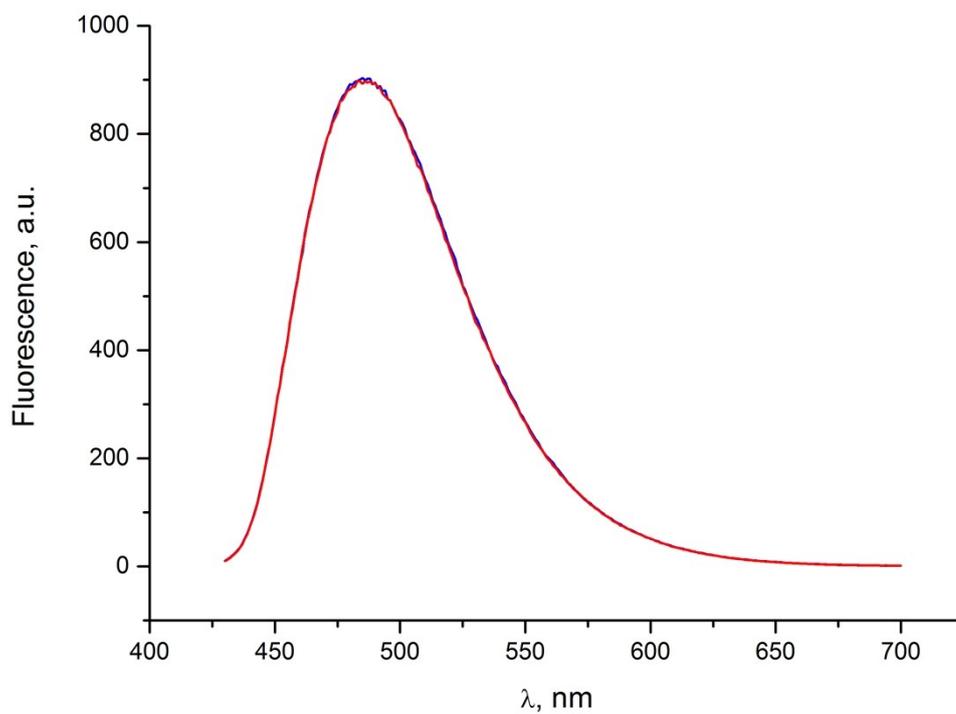
Figure S45. Fluorescence emission spectra of salt **6aH⁺ClO₄⁻** in acetonitrile ($c = 2 \cdot 10^{-5}$ M) before and after addition of 100 eq. PhCF₃.

Table S2. Crystal data and structure refinement for the studied compounds.

| Compound	**5·HBr**	**5·PicOH**	**5·4/3**H_2O	**13**	**6a·HClO₄**	**5·PhOH**
Empirical formula	$C_{18}H_{13}BrN_2$	$C_{24}H_{15}N_5O_7$	$C_{54}H_{44}N_6O_4$	$C_{18}H_{16}N_2O_2$	$C_{38}H_{25}ClN_4O_4$	$C_{24}H_{18}N_2O$
Formula weight	337.21	485.41	840.95	292.33	637.07	350.40
T [K]	120(2)	120(2)	100(2)	120(2)	100(1)	100(2)
Crystal system	Monoclinic	Monoclinic	Triclinic	Monoclinic	Orthorhombic	Monoclinic
Space group	$P2_1/n$	$C2/c$	$P\bar{1}$	$P2_1/n$	$P2_12_12_1$	$P2_1/n$
a [Å]	7.0000(3)	20.993(7)	10.755(3)	4.6952(10)	7.50014(11)	21.179(4)
b [Å]	10.6452(5)	16.920(6)	14.1162(14)	20.135(4)	16.7058(2)	7.3790(15)
c [Å]	18.2521(8)	13.496(5)	15.1222(15)	14.864(3)	22.9329(3)	22.305(4)
α [º]	90	90	117.094(2)	90	90	90
β [º]	98.6140(10)	119.796(6)	99.240(2)	93.406(4)	90	96.923(4)
γ [º]	90	90	90.860(2)	90	90	90
V [Å³]	1344.74(10)	4160(2)	2007.2(6)	1402.7(5)	2873.40(7)	3460.5(12)
Z	4	8	6	4	4	8
D_c [g cm⁻³]	1.666	1.550	1.391	1.384	1.473	1.345
μ [mm⁻¹]	3.050	0.117	0.089	0.092	1.612	0.083
Radiation	MoK_α (λ = 0.71073)	MoK_α (λ = 0.71073)	MoK_α (λ = 0.71073)	MoK_α (λ = 0.71073)	CuK_α (λ = 1.54184)	MoK_α (λ = 0.71073)
No. of reflections collected/ unique	16335/3581	34687/4071	19788/8644	2707/2707	39372/5985	30401/6683
No. of parameters	190	348	577	204	462	495
R indices (all data)	R_1 = 0.0367 wR_2 = 0.0684	R_1 = 0.1716 wR_2 = 0.1758	R_1 = 0.1275 wR_2 = 0.0998	R_1 = 0.0991 wR_2 = 0.1877	R_1 = 0.0423 wR_2 = 0.1055	R_1 = 0.1047 wR_2 = 0.1296
R-factor [%]	2.71	9.36	5.23	8.50	3.93	6.63
CCDC Dep. Nos.	1920000	1920001	1920002	1920003	1920004	1920005